Faculty of Sciences

Sustainable Natural Resources Department

masoto.kelly@studentmail.biust.bw, (+267) 71426441

MULTI-CRITERIA APPROACH FOR FLOOD RISK MAPPING TO SUPPORT FLOOD MANAGEMENT: A CASE OF NATA RIVER BASIN, BOTSWANA

By

KELLY KEFILWE MASOTO

Student ID number: 21100114

BGeom (Geomatics) (UB), MBA (Business Administration) (Heriot Watt), PhD (Business and Management) (UNZA)

A Thesis Submitted to the Faculty of Sciences in Partial Fulfilment of the Requirements for the Award of the Degree of Master of Science in Environmental Science of BIUST

Supervisor: Dr Lenyeletse Vincent Basupi
Department of Earth and Environmental Sciences
Faculty of Science, BIUST
basupiv@biust.ac.bw

May, 2025

Table of Contents

Declaration and Copyright iv
Abstract v
Acknowledgment vii
List of Tables viii
List of Figures ix
List of abbreviations x

Chapter 1 Introduction 1
1.1 Background information 1
1.2 Research problem 5
1.3 Research Aim 7
1.4. Objectives 7
1.5 Research questions 7
1.6 Significance of the study 7
1.7 Operational terms 8
1.8 Project structure 9

Chapter 2 Literature review
2.1 Floods 10
2.1.1 Definition 10
2.1.2 Types of floods 11
2.2 Flood risk 13
2.2.1 Flood risk mapping 13
2.3 GIS and remote sensing 14
2.3.1 Definition 14
2.3.1 Earth observing methods 14
2.3.2 Hydraulic/hydrological approach 15
2.3.3 GIS and remote sensing methods 16
2.4 Delineation of flood extent and water bodies 22
2.5 Botswana and floods 24
2.6 Analysis of Flood Frequency and Return Periods 25
2.7 Gaps in literature 26
2.8 Summary 27

Chapter 3 Materials and Methods 28
3.1 Description of the Study Area 28
3.2 Research Methodology 33
3.2.1 Data Collection 33
3.2.2 Land Use-Land Cover Classification 36
3.2.3 Data analysis 39
3.2.4 Flood extent (Objective 3) 47

Chapter 4 Results and Analysis 49
4.1 Flood frequencies and occurrences 49

4.1.2 Flood frequency analysis 50
4.1.1 Probability of occurrence 51

4.2 Flood risk assessment with gis and remote sensing 54
4.2.1 Elevation and slope 54
4.2.2 Hydrological indicators 60
4.2.3 Land use land cover 66
4.2.4 Soil type 70
4.3 Spatial modelling of flood risk 73
4.4 Sensitivity analysis 76
4.5 Flooding extent mapping 82

Chapter 5 Discussion and Conclusion 85

5.1 Discussions 85
5.2 Conclusion 88
5.3 Further study areas 90

References 91

POSTGRADUATE SCHOOL

Declaration Regarding the Work and Copyright

DECLARATION REGARDING THE WORK AND COPYRIGHT

Candidate: Dr Kelly Kefilwe Masoto

Student ID: 21100114

Thesis Titled: Multi criteria approach for flood risk mapping a case of Nata River Basin, Botswana.

I, the **Candidate**, certify that the Thesis is all my own original work and that I have not obtained a degree in this University or elsewhere on the basis of any of this work.

(If the thesis is based on a group project, then the student must indicate the extent of her / his contribution, with reference to any other theses submitted or published by each collaborator in the project, and a declaration to this effect must be included in the thesis)

This dissertation/thesis is copyright material protected under the Berne Convention, the Copyright and Neighbouring Rights Act, Act. No. 8 of 2000 and other international and national enactments, in that behalf, on intellectual property. It must not be reproduced by any means, in full or in part, except for short extracts in fair dealing; for researcher private study, critical scholarly review or discourse with an acknowledgement, without the written permission of the office of the Postgraduate School, on behalf of both the author and the BIUST.



Signed: ---------- Date: 21/11/2025 ----------

Primary Supervisor Dr Lenyeletse Vincent Basupi

I, the Candidate's **Primary Supervisor**, hereby confirm that I have inspected the above titled thesis and, to the best of my knowledge, it is based on the original work of the candidate.

Signed: ---------- Date: ----------

Abstract

Floods are the most frequent natural disasters, and they have negative impacts on social-economic livelihoods of countries, not forgetting their environment. To effectively manage flood risks and make informed decisions, it is crucial to identify and categorise flood-prone zones. This study predicts flood frequency and suggests a multi-criteria technique for mapping flood risk in Botswana's Nata River Basin. Floods are common in the Nata River Basin and can result in substantial infrastructure damage, fatalities, and financial losses. The suggested method involves integrating multiple criteria, like the soil type, slope, elevation, land use, and hydrographic conditions, to identify areas at high risk of flooding. Satellite images, weather information, and field observations were only a few of the sources used to compile the data for the different criteria. Gumbel distribution was utilised to analyse rainfall data in this study through a period of 31 years. The results of the distribution showed that annual precipitation of 63.28 mm was most likely to occur annually, while 300.59 mm precipitation has 100% probability of occurring every 32 years. Distribution graphs indicated that there is 3% chance of 301 mm rainfall occurring for every year. They also show that there are greater odds of having 63mm, as indicated by exceedance likelihood of 97%. As for objective number two which used Geographic Information System (GIS), ArcGIS Pro, to create a map that shows risk of flooding, the results indicated that an area covering 41.3% of the basin mostly in the southern parts of the study area have high flood risk, while moderate risk was the highest area covering with 54.7% and the low-risk areas covers 8%. Accuracy of the flood risk map was validated through comparison with different AHP scenarios. It was also validated by overlaying it to a flood extent map derived from flooding season satellite images. Most flooded areas from the 2020 floods, according to the flood extent map, fell into the high and moderate risk categories. This indicates

that the GIS-MCA technique serves as a reference for future, more effective flood management and risk decision-making in the basin. The findings demonstrate the effectiveness of the suggested multi-criteria method in identifying locations at high risk of flooding. The strategy is adaptable and can be tailored to the requirements of various river basins in Botswana and other nations facing comparable difficulties. Decision-makers can use the flood risk map produced using the suggested methodology to create efficient flood risk management and mitigation plans. For instance, maps can be used to pinpoint the locations where dredging, building embankments, and other flood control techniques would be most beneficial. The map can also be used to guide decisions on how to use land, such as whether to zone it for residential, commercial, or agricultural purposes.

Keywords: Multi criteria analysis, Flood risk mapping, Flood extent, Nata river basin, Geographic information system.

Acknowledgment

I would like to extend my sincere gratitude to my current supervisor, Dr Lenyeletse Vincent Basupi who took me in at a very critical time of my research, when I would have easily abounded it. Despite my previous supervisor's departure during the most important part of my research, I low key appreciate her (Dr Esther Nelly Lofton (Mosase)) for her guidance and support in making this research successful. I also highly appreciate my colleges Mr Morati Mpalo and Mr Lucky Bongani Moeng on always being available to assist with my ArcGIS hiccups. Above all, I would like to thank God for his grace throughout this study.

List of tables

Table 1	Landsat images metadata	33
Table 2	Required data and their sources.	34
Table 3	Accuracy Assessment for 2020 OLI Image Analysis	38
Table 4	Land cover ranking	43
Table 5	Table showing variables used in Gumbel distribution Model.	49
Table 6	Computation Table of Gumbel's Extreme Value Distribution Method	52
Table 7	Historical Floods Recorded in Botswana with the Rainfall Intensity and Damage Observed	53
Table 8	Land cover distribution across the Nata Basin	67
Table 9	Weighted Overlay Criteria for Study Parameters	74
Table 10	Flood risk map statistics	76
Table 11	Scenarios for sensitivity analysis	77
Table 12	Scenarios for sensitivity analysis statistics comparison	81

List of Figures

Figure 1	Natural disaster types of occurrences in percentage for years 1995-2015 (UNISDR, 2016)	1
Figure 2	Botswana Hazard Impact (2000-2016) Source: (Samuel, 2021).	25
Figure 3	Study area map	29
Figure 4	Nata floods images over the past decade source (social media)	32
Figure 5	Methodology flow chart	35
Figure 6	Flow chart for river basin and stream delineation	42
Figure 7	The AHP process	45
Figure 8	The water cover extent process	47
Figure 9	Total rainfall magnitude-frequency graph for Nata	50
Figure 10	Graph showing the probability of rainfall occurrence	51
Figure 11	Elevation map for the study area	55
Figure 12	Slope map of study area	56
Figure 13	Reclassified Elevation of the study area	58
Figure 14	Reclassified slope of the study area	59
Figure 15	Flow direction in the study area	61
Figure 16	Stream order in the study area	62
Figure 17	Stream Buffer for the study area.	64
Figure 18	Reclassified flow direction for the study area	65
Figure 19	Land use/cover for the study area	68
Figure 20	Reclassified Land use/cover for the study area	69
Figure 21	Soils in the study area	70
Figure 22	Reclassified Soils in the study area	72
Figure 23	Flood risk Map	75
Figure 24. a	Flood risk Maps for scenarios 1.	79
Figure 24. b	Flood risk Maps for scenarios 2.	80
Figure 25	Flood risk levels for scenarios compared in bar chart	81
Figure 26	Water extractions from Landsat images during flooding times 2020	82
Figure 27	Overlay of the flood risk map with flood extent map	84

List of Abbreviations

DEM	Digital Elevation Model
GIS	Geographic Information Systems
CDAT	Change Detection and Thresholding.
SAR	Synthetic Aperture Radar
NASA	National Aeronautics and Space Administration
TM	Thematic Mapper
USGS	United States Geological Survey
RS	Remote sensing
DNDWI	Difference of Normalised Difference Water Indices
RADAR	Radio Detection and Ranging
ETM	Enhanced Thematic Mapper
MFMP	Makgadikgadi Framework Management Plan
ERDAS	Earth Resources Data Analysis System
LULCC	Land Use and Land Cover Change
GPS	Global Positioning Systems
UNISDR	United Nations International Strategy for Disaster Reduction
UNDRO	United Nations Disaster Relief Coordinator
IFRC	International Federation of Red Cross
WHO	World Health Organisation
NDWI	Normalised Difference Water Index
DEM	Digital Elevation Model
GIS	Geographic Information Systems
CDAT	Change detection and thresholding.

CHAPTER 1

INTRODUCTION

1.1. Background of the study

Floods have been said to be the most frequent natural disaster globally (UNISDR, 2015). Figure 1 shows that compared to other disasters, floods occur far more frequently. They have been estimated to account for 43 percentage of all natural disasters specifically weather related between 1995 and 2015, totaling more than 3,000 occurrences that were recorded (UNISDR, 2015). They are abundant, and their destruction compels researchers to thoroughly examine this occurrence (Aroca-Jimenez et al., 2020; Chan, 2022).

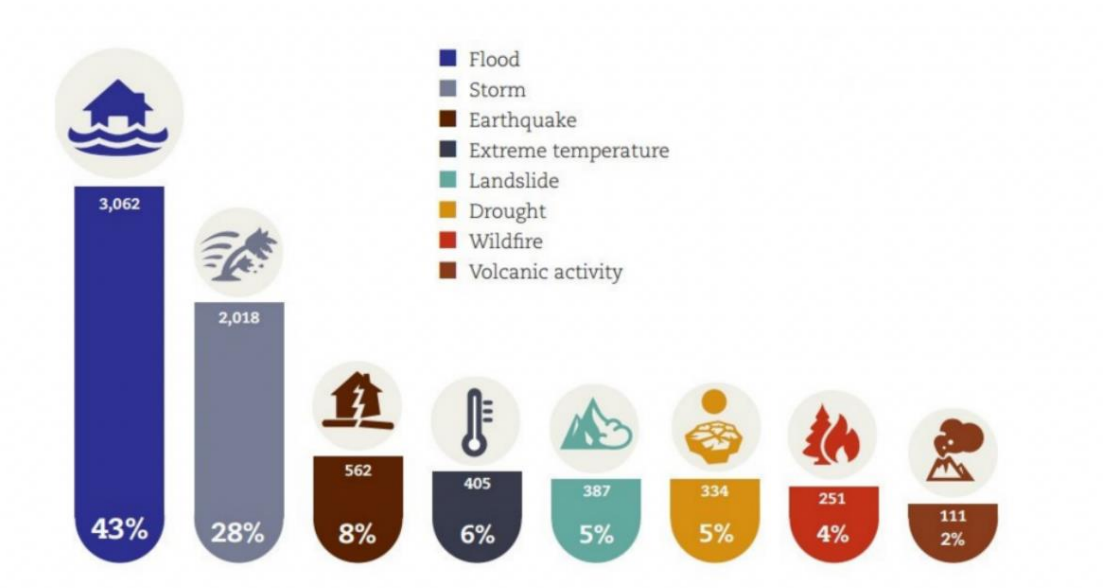


Figure 1: Natural disaster types of occurrences in percentage for years 1995-2015 (UNISDR, 2015)

Introduction

Throughout the world, floods are happening more frequently, becoming more extensive, and costing more resources to repair (Schumann, 2015). Flooding is defined as a temporary situation of partial if not whole inundation of typically dried out areas due to an overflow of inland or tidal waters or from extraordinary and quick backlog or runoff (Natarajan & Radhakrishnan, 2021). Flooding is also described as an overspill of a significant measure of water afar from its normal limits, mainly across an ordinarily dried up terrain (Oxford Dictionary, 2024). Due to a variety of causes, like many other natural disasters, the idea of categorising flooding is preferred.

"1-in-100 year" floods occur every year, primarily affecting developing countries (Renard et al., 2023; Bertola et al., 2020). While floods are predominantly triggered by natural phenomena such as heavy rainfall and storm surges (European Commission, 2007), their impacts are often exacerbated by inadequate housing and infrastructure, ineffective warning systems, low socio-economic status, and a general lack of preparedness within affected communities (Bertola et al., 2020). Additionally, the rapid rise in the effects of floods is attributed to some human activities, such as increasing residential land use, and by lessening the natural retention of water due to land use put together with climate change (Sugianto et al., 2022). The consequences of flooding in areas where no proper and adequate disaster management plan exits get an intense hit to the economy (Tasri, 2021).

To mitigate the impact of these consequences on communities, various institutions have been established, such as the Organisation for the Management of Disasters (OCHA) and the African Region Disaster Management Team (UNISDR, 2016). These entities implement disaster

preparedness measures to address the numerous hydro-meteorological risks faced by many countries. The United Nations Organisation for the Management of Disasters (OCHA) outlines a disaster management structure consisting of five steps, divided into two phases. The first phase covers actions taken before a catastrophic event, while the second phase involves activities following the occurrence of a flood. The pre-catastrophe phase includes preparedness and mitigation/prevention efforts. The post-catastrophe phase encompasses reconstruction, rehabilitation, and disaster relief. These five steps collectively form the disaster management cycle (UNISDR, 2015).

These entities implement disaster preparedness measures to address the numerous hydro-meteorological risks faced by many countries. The United Nations Organisation for the Management of Disasters (OCHA) outlines a disaster management structure consisting of five steps, divided into two phases. The first phase covers actions taken before a catastrophic event, while the second phase involves activities following the occurrence of a flood. The pre-catastrophe phase includes preparedness and mitigation/prevention efforts. The post-catastrophe phase encompasses reconstruction, rehabilitation, and disaster relief. These five steps collectively form the disaster management cycle (UNISDR, 2015).

Other institutions for risk management and monitoring such as, the southern African development community regional platform for the reduction of natural disaster risks, have been established with the acknowledgement of disasters like floods, that have transboundary effects (African Region Disaster Management team, 2010). For the purposes of being prepared, mitigation, response, and rehabilitation, Botswana has a National Policy on Disaster Management

that was endorsed in 1996 (Samuel, 2021). This organisation is also responsible for launching more smaller-scale institutions to carry out the mission at the local level like Botswana Red Cross Society, Botswana Community-Based Disaster Risk Management (CBDRM).

A total of 466mm of rain fell on Botswana in 2000, and five people perished because of floods and strong rains, according to the Pan African News Agency (2000). In January 2013, substantial floods brought about by heavy across Botswana affected approximately 842 households (4,210 individuals), 300 households, and almost 125 households from the Dukwi refugee camp (IFRC, 2013). When 355mm of rain fell in 2013, the intense downpours wrecked houses, buildings, inundated farms, drowned domestic animals and source of living for residents (IFRC, 2013). Additionally, the Cyclone Dineo and subsequent precipitations that impacted southern African region the first few months of the 2016/2017 rainy season left their mark on Nata-Gweta and neighbouring areas (IFRC, 2017). There has been little attempt to identify places at danger of flooding or to define the boundaries of flood severity, despite the enormous impact that floods have on people's lives.

Due to these unattended above-mentioned issues in Botswana’s floods, almost all the villages along the Okavango delta catchment were damaged, including the villages in the Makgadikgadi pans region in the 2010 floods (Mosate, 2010). This continued vulnerability suggests that flood risk information distribution by the appropriate organisation in northern Botswana is of non assistance. Increased urbanisation in flood-prone areas, changes in climate, and population growth are among the key factors contributing to rising flood damage. For example, rapid urban expansion in cities like Jakarta, Indonesia, has led to significant encroachment into

floodplains, exacerbating flood risks (Bertola et al., 2020). Similarly, climate change has intensified extreme weather events, such as hurricanes and typhoons, which cause severe flooding, as seen during Hurricane Harvey in the United States in 2017 (US National Oceanic and Atmospheric Administration, 2018). Population growth in flood-prone areas, such as the Ganges-Brahmaputra-Meghna Delta in South Asia, has increased exposure to flood hazards, amplifying the impact on lives and livelihoods (McGrath, 2017). Botswana has not been an exemption of these causes (Samuel, 2021).

Due to the early reliance on ground surveys for mapping and monitoring floods, these tasks were often constrained by time limitations, accessibility challenges, and adverse weather conditions, which hindered their accuracy and efficiency (McGrath, 2017). For instance, ground surveys during monsoon seasons in South Asia were frequently delayed or rendered inaccurate due to flooding, limiting their utility in real-time flood mitigation efforts. Modern innovations such as Remote Sensing (RS) and Geographic Information Systems (GIS) have significantly mitigated these challenges by providing efficient, large-scale data collection and analysis capabilities. Moreover, computer models that predict and compute exposure offer a cost-effective approach to evaluate mitigation methods, optimise resource allocation, and empower municipalities to collaborate with residents in disaster preparedness (Krichen, 2023).

Recently, the integration of machine learning (ML) and artificial intelligence (AI) has further enhanced these capabilities. For example, AI-based flood forecasting models, such as the one implemented in the Brahmaputra River Basin, utilise real-time hydrological data to predict flood events with greater accuracy, enabling timely evacuation and response (Wagenaar, 2020).

Additionally, ML algorithms have been employed to analyse satellite imagery and identify flood-prone areas more efficiently, as demonstrated in studies conducted in the Netherlands (Wagenaar, 2020). These technological advancements have made it significantly easier to reduce vulnerability to flood disasters compared to earlier approaches."

According to Samuel (2021), spatial technologies can be used to visualise, measure, and analyse floods for a much suitable comprehension of the natural disasters globally. This study will use digital elevation models (DEMs), which offer 3D views to make it easier to perceive flood-prone and at-risk locations, to help overcome or lessen the effects of the observed problem (floods). Building a geographical considerate plan that incorporates locations with high flood risk, how often floods may occur, and their return periods was the outcomes of this research. This would support the nation's disaster management strategy in facilitating the cooperative efforts required during emergencies. Some of the factors that contribute to flooding like elevation or land use in the study area will be taken into consideration when producing the flood risk map (Atanga et al., 2023).

1 .2 Problem Statement

Floods are widely accepted as one of the most controllable natural disasters, yet they remain a significant challenge due to inadequate preparedness and response systems (UNISDR, 2015). While extensive research has been conducted on flood dynamics in Botswana's Okavango Delta basins, including studies on flood risks and mitigation strategies (Wolski et al., 2014; Moses et al., 2023; Gumbricht, 2004), such efforts are scarce for the Nata River basin. Existing studies

predominantly rely on secondary data sources and social or descriptive analysis, with minimal focus on hydrological modelling and GIS-based flood risk mapping.

Despite the availability of advanced tools such as Geographic Information Systems (GIS) and remote sensing for decision-making in flood management, there is no publicly accessible flood risk data specific to the Nata River basin. This gap in data exacerbates the vulnerability of communities near the basin, where at least one settlement faces inundation annually due to environmental changes (IFRC, 2017). The lack of precise flood risk maps limits the ability of decision-makers to mitigate these recurring risks effectively.

Zhai and Lee (2023) emphasise the critical role of Geographical Information and Communication Technology (ICT) in disaster management, including risk reduction, crisis management, and emergency coordination. Yet, Botswana's use of such tools for flood prediction and response remains limited. Consequently, floods continue to surprise communities and overwhelm disaster management systems, often resulting in reactive rather than proactive responses, such as the provision of food baskets and temporary shelters.

This study seeks to address these challenges by focusing on flood frequencies and GIS-based flood risk mapping for the Nata River basin. By applying existing GIS analytical methods, this research aims to provide baseline data on the frequency and magnitude of flooding, enabling better disaster preparedness and decision-making for the region.

1.3 Research aim

The main aim of this research was to examine the frequency of floods and produce a flood risk map that using geospatial techniques in the Nata River basin, Botswana.

1.4. Objectives

a) To ascertain the frequency and occurrence patterns of floods in the Nata River basin.

b) To apply Multi-Criteria Analysis (MCA) in conjunction with geospatial techniques to generate flood risk maps and flood inundation maps for the Nata River basin, with particular focus on the 2020 flood event.

c) To investigate mitigation measures and propose sustainable strategies for managing floods in the Nata River basin, aligning these with the context of a developing country scenario.

1.5 Research questions

a) What is the frequency and pattern of flood occurrences in the Nata River basin?

b) How can Multi-Criteria Analysis (MCA) and geospatial techniques be utilized to develop accurate flood risk and inundation maps for the Nata River basin?

c) What sustainable flood mitigation measures can be proposed for the Nata River basin to inform policy and enhance decision-making at various governance levels?

1.6 Significance of the study

This study produced a flood risk and extent map for Nata River basin with the use of ArcGIS Pro. The creation of these maps can assist the government and public of the Nata - Gweta region villages to come up with effective flood damage reduction that can be used long term in the region.

The identified departments, such as the Department of Environmental Affairs, Department of Water Affairs, and Department of Lands, may view this approach as a valuable tool for managing and enforcing their solutions to minimising flood risks, safeguarding the environment, offering insurance solutions, and organising sustainable development initiatives. Construction rules, zoning laws, and subdivision bylaws are a few examples of the tools that can be used to regulate land use within flood risk zones. With all of them in place, the extent of flood damage would be reduced if flood plains were set aside for purposes like parking lots, recreational spaces, and agricultural pursuits that are less vulnerable to flooding damage. All in all, this inundation maps and tool to predict where to attend a flood crisis first will not only benefit the Village Development Committee, which is the first response and planning authority in most villages, but also the Land Boards and Department of Town and Country planning.

1.7 Operational terms

a) **Flood** "to let water fill or cover a space, especially when it does so in a way that causes issues, according to the oxford dictionary."

b) **Risk** the likelihood of losing anything, which is determined by three factors: the degree of danger, the ease with which something can be damaged, and the amount of exposed area.

c) **Vulnerability** The capacity to suffer harm or impairment. It speaks to the likelihood that floods will have an impact on lives, infrastructure, and the economy. The amount and kind of buildings, demographic characteristics (such as age and health), land use, and the capacity to anticipate and prepare for floods are some of the factors that affect susceptibility.

d) **Hazard** the likelihood that a region would be impacted by a potentially catastrophic natural catastrophe, such as a storm or earthquake.

e) **Inundation** A flood or the condition of being flooded with water.

1.8 Project structure

The dissertation is organised into five chapters. Chapter 1 introduces the study, which focuses on analysing the frequency of floods and utilising modern geospatial tools to create a flood risk map for the Nata River basin in Botswana. This chapter also includes the problem statement, aim and objectives, background information, and the significance of the study.Chapter 2 provides a comprehensive literature review, discussing types of floods, methodologies for mapping flood risks, and empirical studies on GIS-based flood risk mapping.

Chapter 3 outlines the methods of data collection and analysis employed in the study. This includes land use and land cover classification, techniques for flood extent mapping, and validation processes for the geospatial methods used. Chapter 4 presents the results, which are organised under the subheadings: flood frequencies and occurrences, geospatial flood risk assessment, and flood extent mapping. Finally, Chapter concludes the dissertation by summarising the findings and providing recommendations for managing flood risks in the Nata River basin.

CHAPTER 2

LITERATURE REVIEW

2.1 Floods

2.1.1 Definition

Floods are the most well-known of all natural disasters of the world, it frequently claims over 20,000 lives year in year out and has an impact on nearly seventy-five million people around the world (Samuel, 2021).

The definitions associated with flooding are vast and do have different meanings to each researcher with respect to the context and location of their study (Andráško, 2024). Gogoi & Patnaik, 2022, defined flooding as the occurrence of more water entering a drainage channel than it can move. The surrounding areas become inhabitable because of the access water spreading out and flowing over the banks.

Water that collects above ground because to high tides, strong rainstorms, or quick runoff from concrete surfaces (Gogoi & Patnaik, 2022). Natural floodplains are part of most of the rivers. Most of the extreme floods occur along the coastal regions. Such regions have a combination of substantial precipitation and poor soil which make them more prone to flooding.

McCormack et al, 2022 established that there are several components used in depicting the extent of flood and its nature. They are determined by several variables, including duration of

flow, the amount of space it covers, the speed of that flow, and the amount of water discharged over time. Season of the year (rainy season or dry season), Rainfall, topography, together with soil type and geomorphic features all have an impact on these variables. Most of the increasing flood events are due to increased human population, the changes in land-use pattern and climate change (McCormack et al, 2022).

2.1.2 Types of floods

2.1.2.1 Coastal (Surge) flooding

This type of flood is attributed to extreme storm occurrences, this is because they bring large waves and strong onshore coastal winds together with high tides that fill bays and coastal zones with ocean water (Renard et al., 2023; Bentivoglio, 2022). This type of flooding is characterised by the upsurge in sea level beyond conventional tidal altitudes caused mostly by low air pressure and storm feat over a large area of open water which is known as a storm surge. A dome of water is produced during a storm or hurricane due to suction, which is caused by low tension inside the storm's eye (Bentivoglio, 2022).

2.1.2.2 Fluvial (Riverine) flooding

These are brought about by long time of rainfall in a catchment area that leads to a steadily rising water level that eventually overwhelms the river's banks (Bentivoglio, 2022). They are mostly known to be slow speed moving floods so they do affect largely inundated zones that can damages but not many fatalities (Renard et al., 2023).

Flash floods like other rapid flooding events are more common on smaller rivers, rivers with steep valleys, rivers that flow over impermeable land cover for a significant portion of their course, and generally dry channels (Bentivoglio, 2022). The reason could be because of an abrupt or sudden discharge from an upstream impoundment formed behind a dam, a glacier, or a landslide, or it just be a localised continuous rainfall (strong thunderstorms) (Bentivoglio, 2022). Riverine flooding can be classified into two categories: over-bank flooding and flash flooding.

2.1.2.3 Pluvial (Surface Water) flooding:

This type of flooding occurs when rainfall water starts to collect in a low elevated location which has clayey soil types (Renard et al., 2023). It can be easily predicted. Surface runoff happens when the amount of rainfall exceeds the soil's capacity to permeate and evaporate, or when the ground cover is impermeable (WMO, 2013). The utilisation of a closed passage system to collect and use of extra surface runoff water following rainfall is the concept behind avoiding this type of flooding. According to this theory, the system should be able to retain and remove runoff regardless of how much rain falls or how long it lasts (WMO, 2013).

2.1.2.4 Urban flood

These types of floods can be caused by all of the above-mentioned type of floods if they occur in a urban area. Urban flooding is frequently caused by excessive precipitation combined with impermeable surfaces that happen to have poor drainage. Because most metropolitan areas in developing countries have concrete surfaces with little soil and inadequate drainage systems, the

rain that falls cannot properly run away. (Eldho, 2018). This ailment is recognised for its recurring and comprehensive impact on the region, irrespective of proximity to or placement within a floodplain or aquatic body (Renard et al., 2023).

2.2 Flood risk

It is common for people to use risk and hazard interchangeably. However, risk is defined as the likelihood of a harmful outcome such as personal injuries, deaths, means of livelihood and economic loss because of the interaction between hazards and vulnerability (UNISDR, 2008). Studies undertaken by Antzoulatos et al., (2022) and Ganjirad et al, (2023) characterised flood risk because of flood hazard and susceptibility. They then describe Risk as '*the uncertain product of a hazard and its potential loss*'.

2.2.1 Flood risk mapping

The mapping of floods has been done using several varying methods or techniques (Antzoulatos et al., 2022). These include the utilisation of airborne remote sensing (RS), traditional ground survey, and models of hydrodynamics. Hydrodynamics refers to the study of the motion of fluids, particularly water, and the forces acting upon them. In the context of flood mapping, hydrodynamic models simulate water flow and its interactions with terrain and infrastructure. These models are significant because they allow for the accurate prediction of flood extents, flow patterns, and the impact of various flood scenarios, providing critical insights for risk assessment and mitigation planning.

Accessing and getting spatial data from widely dispersed floodplain areas for flood risk mapping is time consuming and expensive. Then the introduction of remote sensing has made this

challenge less of a worry. Satellites equipped with sensors of optical and/or microwave have provided a synoptic view over large areas which has been helpful for flood mapping (Bentivoglio, 2022). There is a work by Rachael et al. (2015) that used Landsat TM imagery to track flooding in the varied floodplain wetlands of the Macquarie Marshes, Australia, which is an excellent example of where this remote sensing technique was helpful. One of the biggest semi-permanent freshwater wetlands in the region, the marshes span 19,850 hectares in South-east Australia, which means mapping floods in such an area was a very beneficial undertaking for the community.

2.3 GIS and remote sensing

2.3.1 Definition

In recent years, it has been demonstrated that geographic information systems (GIS) and remote sensing (RS) technologies are valuable tools for mapping and monitoring floods (Jonah, 2024). These decision support tools are primarily concerned with creating flood maps (risk/hazard) for places that are at risk and with defining flood zones.

An information system that is intended to gather, store, process, and present spatial data is known as a geographic information system (GIS) (Lillesand and Kiefer, 2014). Flood mapping and disaster management scenarios have been said to be well carried out through GIS because of their spatial component (Saikh et al., 2023). On top of having visualisation capacity GIS in flood mapping does also provide spatial analysis tools to assist in estimating how much damage and risk an area is vulnerable to. For RS, images acquired before, during and after a flood from satellites

are beneficial in deriving the extent and intensity of the flood event. Appropriate mitigation and flood relief plans can also be deduced from these images.

2.3.2 Earth observing methods.

Samarasinghe et al.'s (2010) work in the Kalu-Ganga River, Sri Lanka, demonstrates how earth observation techniques, including hydrological and hydraulic models, have been successfully applied to mapping and flood risk analysis. In order to ascertain the flood range, two satellite images taken during the dry season and during flooding were analysed. The findings demonstrate that the flood extent they calculated from the data was similar to the data gathered when one of the flood models was used, and they were able to validate their model as a result. The study also made use of GIS data and tools for risk mapping and flood simulation. Samarasinghe et al. (2010) were able to map out high, medium, and low flood risk zones by overlaying vulnerability and flood hazard values with the region's polygon map in a GIS context.

2.3.3 Hydraulic/hydrological approach

The hydrological approach's benefit is that it generates extremely exact and thorough results that are necessary for correct risk assessment and hazard mapping; however, its disadvantage is that it necessitates proper and adequate field surveys and gauging stations that can gather the data required for accurate risk calculation (Afzal et al., 2022).

The contribution of conventional hydrological monitoring systems to emergency response, mapping, and flood forecasting is less. The expense of keeping up rain and stream gauge stations can be an issue in most nations. (Poudel, 2021). The difficulties of maintaining these stations are

increased in circumstances when there are gaps in the hydrographic time series caused by out-of-service stations. Additionally, rivers are frequently shared by nations; as is well known, information on floods in upstream nations is not usually shared with downstream nations due to transboundary rivers. This is another challenge to using this method for downstream countries since some of these upstream floods affect flow downstream which is needed as an input in some models (Afzal et al., 2022; Poudel, 2021).

Countries must be able to independently gather information across borders in order to provide sufficient flood warnings. Conventional hydrological monitoring systems, such as gauging stations, are critical for recording water levels. These stations, however, primarily measure the height of the water at specific locations rather than providing information on the overall extent or impact of a flood. This limitation underscores the need for complementary methods, such as remote sensing and GIS, to capture a more comprehensive understanding of flood dynamics. For regions the size of Botswana and most of the southern African nations, where hydrological data are either nonexistent or extremely erratic. These aspects cause problems for hydrologic models, which are the standard method used in flood predictions; this makes applying these techniques challenging.

2.3.4 GIS and remote sensing methods

In these methods there is need to look at more than one image or map of the area of interest to see the difference without the need to go to the area physically, even though it would be advisable to go and ground truth your product so as to validate it. The below mentioned are the

form of data needed in detecting the change in the images or maps. This method of mapping floods is mostly based on change detection (Akinyemi, 2021).

Change detection uses multi-temporal satellite imagery to identify variations in geographic features or land characteristics caused by artificial or natural phenomena. According to Lillesand and Kiefer (2014), it is crucial for remote sensing, monitoring environmental changes, and analysing alterations in land use and land cover. For the purpose of detecting changes, remote sensing satellites capture images of the Earth at varying time intervals and spectral bands, which enable detailed analysis of environmental and land use changes. Due to its widespread application, change monitoring which entails identifying changes in photos of the same region taken at different times is extremely important (Alawadi et al., 2023).

Using synthetic aperture radar (SAR) data and change detection and thresholding (CDAT) techniques, Long et al. (2014) mapped the flooding extent on the Chobe floodplain in Namibia's Caprivi area. They used adaptive filtering, segmentation, decision-based classification based on threshold values, and image differencing in their methodology. To determine the areas that were flooded during seasonal floods, these techniques were applied to data from the ENVISAT/ASAR and Radarsat-2 satellites. This method has benefits since satellite data, like Landsat, is readily available. It may be used for large-scale flood mapping without requiring extremely accurate inputs or computationally demanding procedures, which can help with flood risk management.

2.3.4.1 Optical data

Optical sensors in Geographic Information Systems (GIS) play a crucial role in flood mapping by detecting natural energy reflected or emitted from the Earth's surface, particularly in visible and infrared spectral bands. In areas where water surfaces are unobscured by clouds, trees, or floating vegetation, high-resolution visible/infrared sensors offer precise delineation of inundated regions, as highlighted by Lillesand and Kiefer (2014). Notably, near-infrared imagers prove highly effective due to the strong absorption of near-infrared spectral bands by water and their reflection by land, as noted by Klemas (2015).

Optical remote sensing finds innovative applications in flood mapping, as demonstrated by Ogashawara, Curtarelli, and Ferreira (2013). Their study utilised the Difference of Normalized Difference Water Indices (DNDWI) derived from medium-resolution Landsat 5 TM surface reflectance data captured before and after Hurricane Ike in 2008. By employing a threshold analysis approach and integrating data from the USGS mobile storm surge network, they accurately identified flooded areas, achieving an 85.68% accuracy for flooded areas and 92.13% for unflooded areas. However, further investigations are warranted to understand the spectral response of vegetation in flooded regions.

The catastrophic floods of the Mississippi and Missouri rivers in 1993 underscored the utility of satellite sensors for surveying vast flooded areas. This historic event, which caused extensive damage and loss of life, was extensively studied using satellite data, including Landsat 5 TM imagery. NASA utilised pre- and post-flood data to map the flooded regions, showcasing the effectiveness of satellite sensors during large-scale flood events.

Righini et al. (2024) proposed an efficient and cost-effective method for mapping flooding in coastal floodplains based on Landsat 7 TM imagery and Digital Elevation Model (DEM) data.

Despite challenges in locating flooded areas beneath dense vegetation canopies, their method proved reliable, with validation through ground observations. However, the reliance on river gauge measurements poses limitations, making this method less suitable for flood mapping in regions like Botswana due to associated costs.

2.3.4.2 Synthetic aperture radar (SAR) data

Synthetic Aperture Radar (SAR) technology, distinguished by its independence from solar electromagnetic energy or terrestrial thermal properties (Anusha & Bharathi, 2020), stands out in flood mapping due to its versatility and reliability. Unlike optical sensors, SAR is not constrained by daylight or weather conditions, making it an invaluable tool for mapping floods across various environmental contexts. Its utilisation of the microwave band enables SAR to penetrate through obstacles such as clouds, vegetation, rain, fog, and snow, ensuring consistent data acquisition even in challenging conditions (Hernández-Hamón, 2023; Klemas, 2015; Anusha & Bharathi, 2020).

Moreover, SAR's capability to differentiate between land and water surfaces adds another layer of effectiveness to its flood mapping prowess. This ability stems from SAR's detection of variations in surface roughness, which allows it to distinguish between flat water surfaces and other land features. As a result, water bodies appear as darker pixels in SAR imagery compared to non-water areas, providing clear contrasts essential for accurate flood mapping (Gan et al., 2012).

Numerous studies underscore the utility of SAR data in flood monitoring and mapping applications. For instance, Honda, Francis, and Sah (1997) successfully utilised JERS-1 SAR data to extract flood-affected areas in Thailand, showcasing SAR's effectiveness in capturing flood

dynamics. The capacity of SAR to provide continuous and timely information, unaffected by atmospheric conditions, makes it a preferred choice for flood monitoring initiatives (Dewan et al., 2014). However, challenges persist in accurately delineating flooded areas, particularly in the presence of rough water surfaces, emergent vegetation, or rapidly moving water, which can complicate interpretation (McCormack et al., 2022).

De Groeve (2010) provides a comprehensive overview of the utilisation of passive microwave observations for the detection, mapping, and sizing of floods.. These observations enabled the detection of floods within as little as two hours after their occurrence. By observing upriver areas, early warning systems with start times of up to 30 days became feasible. Although the flood maps generated were of poor quality compared to now maps, they aligned closely with maps derived from higher resolution imagery. Daily data availability facilitated a deeper understanding of flood dynamics and enabled objective flood sizing through the integration of temporal and spatial information. These methods were applied to investigate southern Africa floods in 2009 and flood season for the year 2010 in Namibia specifically (De Groeve, 2010). Similarly, Townsend (2002) analysed Radarsat scenes from 1996 and 1998 to portray flood cover in Roanoke River floodplain forest which is in North Carolina, demonstrating SAR's capability to monitor and map flood events.

In another study Townsend and Walsh in (1998) looked around the lower laying areas of Roanoke River floodplain, still in the North Carolina region, GIS models demonstrating likely flood inundation and moisture were generated using Digital Elevation Models (DEMs). Additionally, SAR images from satellites were employed to identify potential flood risk. While

both the SAR images and GIS model provided analogous results of the flood occurrence, the method's accuracy heavily relies on the precision of the DEM. In cases where highly accurate DEMs are unavailable, such as in comparatively flat areas, different dates SAR and optical remote sensing can serve as viable alternatives, provided they offer sufficient temporal resolution to capture the flood event (Alawadi et al., 2023).

Stereo interferometry can be exploited to precisely generate Digital Terrain Models (DTMs) from stereo pairs of RADAR pictures. These DTMs are essential spatial datasets that are used for creating hydrological models for assessing the risk of flooding, together with Digital Elevation Models (DEMs). They make it easier to define water catchment areas, identify watercourses, identify accumulation points, and anticipate stream flow, which makes it possible to forecast the occurrence and spatial distribution of flood incidents (Leon et al., 2013).

Additionally, the creation of high-density last return point surfaces is made possible by the growing usage of Light Detection and Ranging (LiDAR) photography, which helps to produce extremely precise DTMs. By providing comprehensive topographic information necessary for efficient flood modeling and prediction, this cutting-edge technology improves the accuracy and detail of terrain modeling, thereby making a substantial contribution to flood management and risk assessment techniques (Leon et al., 2013).

Sanyal and Lu (2004) offer an example wherein they distinguished between inundated and non-inundated areas in India by combining SAR data with Landsat Enhanced Thematic Mapper Plus (ETM+) imagery. Limitations like data cost and long revisit times remain obstacles, especially

when it comes to delineating flood extent during peak events or tracking flood progression, even though the research emphasised common challenges in precisely obtaining information from SAR imagery in flood prone areas (Sanyal & Lu, 2004).

2.4 Delineation of flood extent and water bodies

Various techniques have been developed specifically for mapping standing water, such as single band density slicing (Keagakae, 2020), supervised and unsupervised classification (Lambin et al, 2003; Sebego et al., 2019), and spectral water indices and band ratios. Among these methods, spectral water index techniques stand out for their reliability, user-friendliness, efficiency, and cost-effectiveness in computation (Lambin et al, 2003). Numerous water indices have been created throughout the previous few decades. The most commonly used of these are the Modified Normalised Difference Water Index (MNDWI) by Xu in 2006 and the Normalised Difference Water Index (NDWI) by McFeeters in 1996. One of the earlier contributions in this field is the Normalised Difference Water Vegetation Index (NDVI), which was put forth in 1974 by Rouse and associates.

2.4.1 The normalised difference water index

An index that is produced from remote sensing and used to track changes in the water content of water bodies is called the Normalised Difference Water Index (NDWI). McFeeters defined it as follows in 1996:

$$NDWI = (green - NIR) / (green + NIR)$$

The Normalised Difference Water Index (NDWI) plays a pivotal role in identifying and monitoring water bodies. Numerous studies have refined the NDWI framework to enhance the accuracy of water extraction. For example, by combining radar backscattering coefficients with NDWI, the SAR and Optical Imagery Water Index (SOWI) was developed, facilitating precise water boundary delineation across various scenarios (Keagakae, 2020). Furthermore, integrating NDWI with thermal infrared data and surface energy balance components has proven effective in assessing plant health, crop conditions, and water availability in agricultural contexts (Lambin et al, 2003).

Additionally, NDWI has been utilised to estimate the construction timeframe of road bridges, contributing to bridge management systems and informed decision-making regarding maintenance and preservation strategies (Lillesand and Kiefer, 2014). These diverse applications underscore the versatility and importance of NDWI in fields ranging from water resource management and agriculture to infrastructure maintenance.

2.4.2 The modified normalised difference water index

The MNDWI adjusts McFeeters' NDWI by substituting the Near Infrared (NIR) band for the Shortwave Infrared (SWIR) band, which helps differentiate water characteristics more clearly. Lillesand 2014 says that the MNDWI is more appropriate and less prone to shadow noise. for defining aquatic bodies in the presence of populated regions, when the addition of the SWIR band effectively lessens the noise from populated areas throughout the NDWI. MNDWI's assortment

of wavelength bands uses the green wavelength to boost the coefficient of reflection of water characteristics and the soil's strong SWIR coefficient of reflection to offset the low SWIR reflectance of the water features (including vegetation) (Lillesand and Kiefer, 2014).

However, it has been suggested that using the green wavelength may skew the results of the water index because flora has a higher green coefficient of reflection than nearby non-water characteristics such bare land and soils (Keagakae, 2020; Lillesand and Kiefer, 2014). In Keagakae's (2020) alternate version of the MNDWI, the Red wavelength band is replaced with the Green band when using the Moderate Resolution Imaging Spectro-radiometer (MODIS) optical sensor. When mixed cells (pixels) from wetland and dry land areas are present, this MNDWI has been shown to be surface water sensitive and reduces the impact of reflectance from green vegetation.

2.5 Botswana and floods

Botswana has a medium level of disaster risk, according to the Inform Global Risk Index. The primary causes of flooding there are storm surge from tropical cyclones, unexpected and heavy rainfall, strong precipitation, and dam overflow leading to spillage (European Commission, 2018). In order to provide knowledge about flood disasters and provide legal backing for related actions, Botswana lacks a dedicated statute (NDMO, 2009). Figure 2 indicates that most people in Botswana are affected by floods than any other disasters hence the need for proper disaster risk management set ups.

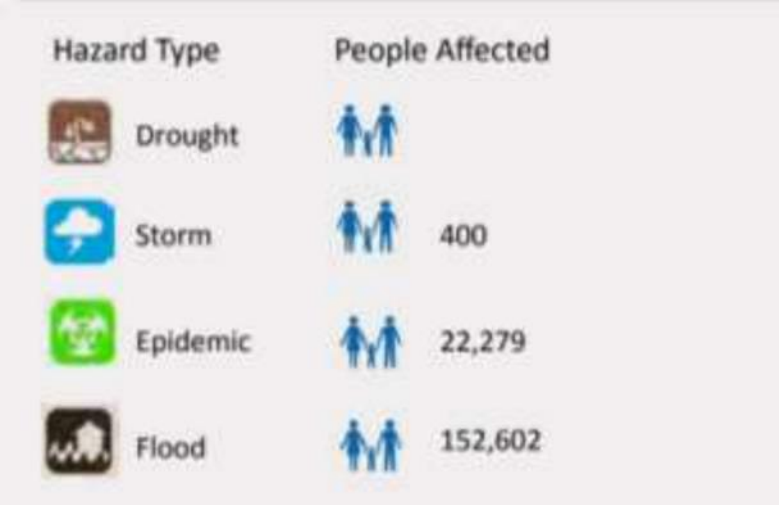


Figure 2: Botswana Hazard Impact (2000-2016) Source: (Samuel, 2021).

2.6 Analysis of flood frequency and return periods

Flood frequency analysis is the method of determining how frequently a specific event would occur in order to predict the extreme occurrences with a wide recurrence interval (Bhagat, 2017). For example, with this technology, floods every 10 years, 20 years, 50 years, and 100 years can be projected. These forecasts are made possible by statistical frequency curves for floods, such as the Gumbel curve, which offer accurate estimates of the frequency of floods (Samuel, 2021). In order to safeguard the public, these estimations are crucial for controlling floodplains and for designing roads, bridges, culverts, dams, and industrial buildings (Bhagat, 2017).

Extreme precipitation occurrences have a positive correlation with total precipitation levels, according to research by Mashao et al. (2023). Because of this, excessive precipitation plays a significant role in the frequency of flash floods in Nata, making total rainfall a suitable metric for examining the frequency of flooding in the area. This study aims to close the gap in the literature by conducting the first flood frequency analysis study in Botswana. Flood frequency

analysis often makes the assumption that the maximum yearly floods are independent, random events with a uniform distribution that are static. Nonetheless, annual maximum floods are dynamic in the context of climate change (Mashao et al., 2023).

In order to facilitate the design and development of the country's infrastructure, as well as the recovery phase of the disaster management cycle, it is imperative for nations to take into account the probability, magnitude, frequency, and estimated return durations of distinct floods.

2.7 Gaps in literature

The use of geospatial risk assessments for flood disasters is not been highly used by the disaster organisations in Botswana, as is information on the frequency and magnitude of floods. This claim is substantiated by studies such as Madzudzo et al. (2018), which reveal limited use of GIS for flood vulnerability analysis in regions like Ramotswa and Taung. Furthermore, the National Disaster Management Office's Hazard Identification, Vulnerability, and Risk Assessment underscores the need for advanced methodologies, noting a lack of structured integration of GIS in disaster planning. Similarly, the World Bank's ThinkHazard Report classifies Botswana’s urban flood risks as high, yet emphasises the absence of geospatial tools in current risk assessments and planning. The lack of geospatial technologies in flood management poses significant challenges. Without accurate spatial mapping, it becomes difficult to identify high-risk areas, hindering effective mitigation strategies. This gap also impacts disaster preparedness, leading to insufficient forecasting and delayed emergency responses.

2.8 Summary

This literature review examines the definition and types of floods, flood risk assessment, and the application of GIS and remote sensing in delineating flood extents and water bodies. It highlights the specific challenges faced by Botswana, where limited research on flood magnitude, frequency, and geospatial risk assessments exists due to its semi-arid environment. The review underscores the importance of using geospatial technologies and analysing flood frequency and return periods. Notably, it identifies significant gaps in existing literature, emphasising the need for comprehensive studies and advanced technological applications to better address flood risks in Botswana.

CHAPTER 3

MATERIALS AND METHODS

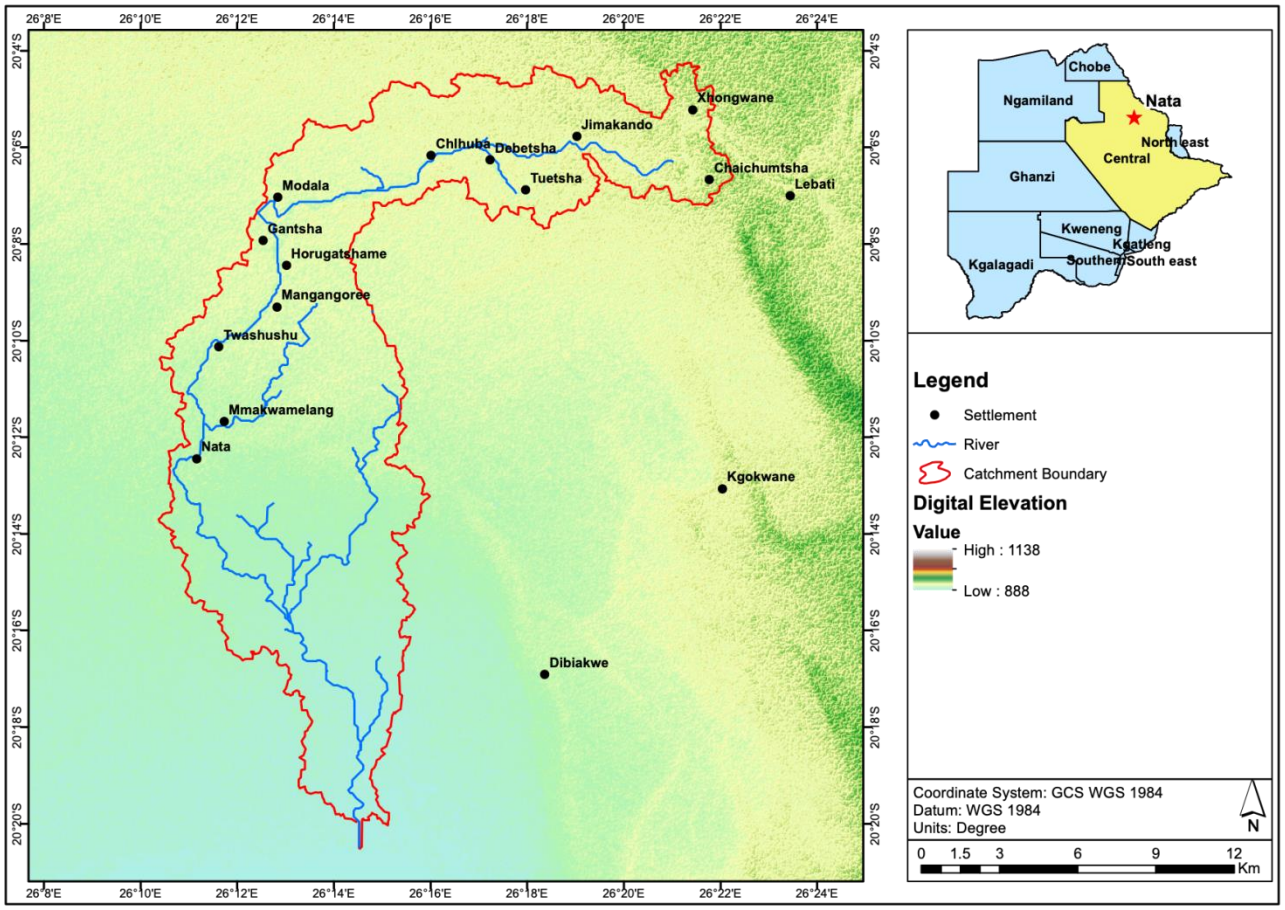
3.1 Site description

3.1.1 Location

The Makgadikgadi Pans are located in northeastern Botswana, south of the Chobe River front and southeast of the Okavango Delta, two of the country's most popular tourist destinations. The Nata River system allows the Makgadikgadi Pans' wider catchment area to flow into Zimbabwe to the east and north. Through the Boteti River, it is also connected to the Okavango system on the northwest side. The Sua Pan on the east and the Ntwetwe Pan on the west make up the wetland area, both of which are governed by the SADC Shared Water Courses Protocol. This protocol is an agreement among member states of the Southern African Development Community (SADC) that promotes sustainable management and cooperative development of shared water resources. Its relevance lies in emphasising the importance of cross-border collaboration in managing the hydrological and ecological characteristics of the pans, ensuring equitable resource use and flood management.

The eastern Sua Pan basin receives inflows from the Makgadikgadi Basin's Nata River as well as the Mosetse, Semowane, Lepashe, and Mosupe Rivers. The focus of the study is this portion of the Pans. The study's geographic location in respect to the nation is depicted on the map below. Given the multitude of river systems present in the western portion of the

Makgadikgadi, the author opted to concentrate on just one system in order to minimise laborious work that could result in an unachievable goal for the study period. The primary study region is



the Nata River system (figure 3).

Figure 3: Study area map

3.1.2 Relief and drainage

Aeolian erosion and soil transport have an effect on the soil structure and sensitivity of the Kalahari sandveld, according to a research conducted for the MFMP. They also increase the salinity of the groundwater downstream from the pans and provide nutrients and salts to the adjacent grasslands. They also exert a substantial influence on the system's topography and the pan surface's Aeolian deflation.

When mapping drainage lines, especially east of the Pans, the study finds that margin suggests two distinct patterns or zones of drainage. The majority of rivers are well-incised above the 1000 m contour and have a dendritic surface structure. Below the 1000 m contour, the Semowane, Mosetse, Lepashe, and Mosupe Rivers enter the area of the ancient lake floor through restricted floodplains. This area has a higher potential for infiltration because of its calcareous and silica karst architecture. Below the 1000 m contour, the watersheds between these rivers are broad and flat, and they could serve as direct recharge zones for the Pan basin. A variety of riparian wetlands and delta systems are supported by the channel's widening flood plains as it approaches the Pan and its shallow discharge.

3.1.3 Vegetation and climate

The spatial extent of six main vegetation types saline grasslands, shrubbed grasslands, mixed mophane shrubbed woodlands, mixed acacia shrubbed woodlands, mixed terminalia shrubbed woodlands, and mixed combretum shrubbed woodlands was identified by a broad vegetation classification that was developed and mapped for the Makgadikgadi Framework Management Plan (MFMP) area. Focused field sampling and GIS analysis of Landsat photos served as the foundation for this classification.

For every decade, as well as a 2–3-year time scale, significant inter-annual rainfall fluctuations take place. As a result, inter-annual variability is very noticeable, with a large divergence from the mean across the whole study area. The wettest months on average on a monthly basis are January and February, whereas the driest months on average on a yearly basis are July and August, with average evapotranspiration rates above 2 500mm.

Extreme rainfall episodes in the Makgadikgadi basin are closely associated with both SST (Sea Surface Temperature) anomalies in the Indian Ocean and Enso (El Nino Southern Oscillation) cycles in the Pacific. For example, records for the 1980–2000 time series showed a strong correlation between the wet season rainfall (December–February) in the Nata River Catchment and the SIOD levels for January–March of the same year. Furthermore, there is a connection between significant rainfall events and the landfall of tropical storms during La Nina conditions and the ensuing anomalous low-level moisture transport into eastern southern Africa.

3.1.4 Brief historical account of floods in the area

The annual flooding of the pan surface that results in the formation of large salt lakes is caused by a mix of input from rivers, direct rainfall, and local drainage during the rainy season. On the other hand, the eastern river floods are often the region's ephemeral river flows; brief floods with a sharp peak that are timed with precipitation and normally peak in January and February. Nata and the surrounding areas experience floods almost every year during the rainy season. For instance, in March 2017, Mmegi reported that some people had to be airlifted from their homes due to severe flooding. Additionally, the United Nations Office for the Coordination of Humanitarian Affairs (OCHA) reported in March 2016 that rivers in Sepako, a village near Nata, were flooding, causing significant disruptions to movement and daily activities. In January 2013, torrential rainfall between the 16th and 23rd caused extensive flooding in the Central Province of Botswana. Villages in the Tutume Sub-District, including Zoroga, Tsokootshaa, Nata, and Sowa, were significantly affected. According to ACMAD (2013), at least 842 families (approximately 4,210 people) were impacted by the floods, which included 125 refugee families and 300 displaced families. The deluges wrecked roads, houses, crops, inundated dams, animals,

and means of subsistence (ACMAD, 2013). In March 2018 Mmegi newspaper reported a trail of destruction by the floods surrounding Nata. Every year rainfall seems to leave a trail of disaster for Nata as seen in the images in figure 4, hence the need for a study as this.



Figure 2: Nata floods images over the past decade source (social media)

3.2 Methodology

3.2.1. Data Collection

For the study periods, Landsat satellite missions providing Thematic Mapper (TM), Enhanced Thematic Mapper Plus (ETM+), and Operational Land Imager (OLI) with Thermal Infrared Sensor (TIRS) capabilities provided cloud-free and radiometrically corrected Level 2 multi-temporal satellite images. These photos were obtained from the U.S. Geological Survey's (USGS) Earth Resources Observation and Science (EROS) Center Science Processing Architecture (ESPA) webpage (http://earthexplorer.usgs.gov/), and they include surface reflectance data at a spatial resolution of 30 meters (as indicated in Table 1). Table 1 provides a comprehensive overview of the information for all the multi-temporal satellite pictures taken over the different study periods.

The primary objective of collecting these images was to address the study's goals of applying geospatial and Multi-Criteria Analysis (MCA) techniques to create flood risk and inundation maps (with a focus on the 2020 flood event). Each satellite system offered unique capabilities that distinguished it from the others. The TM provided foundational spectral bands for analysing surface reflectance and hydrological features, ETM+ enhanced the spectral and radiometric resolutions to improve feature detection, and OLI/TIRS incorporated advanced thermal and reflective capabilities for detailed flood extent and risk mapping.

Table 1: Landsat images metadata

Satellite	Sensor	Spatial resolution (m)	Date of caption

Landsat 8	OLI/TIRS	30	2 to 18 February 2015
Landsat 8	OLI/TIRS	30	1 to 31 January 2020

The purpose of this dissertation is to produce a map that shows the risk of flooding in the Nata River basin using remotely sensed data in an ArcGIS environment. To determine possible contributing variables to local floods, site inspections were carried out throughout the research region. Using Multi Criteria Analysis (MCA), flood-prone areas are located. Flood risk was shown to be influenced by rainfall intensity, land use/cover, slope, geology (soil type), elevation, and flow accumulation. Digital Elevation Models (DEMs) and satellite data were downloaded from the USGS Earth Explorer platform. With the primary goal of assessing flood risk based on topography, the DEM was used to depict the terrain in three dimensions through maps. For the objective of mapping flood risk, the SRTM digital elevation model encompassing the catchment region surrounding the study site at a spatial resolution of 30 meters was combined with the satellite pictures that were gathered. ArcGIS pro software was used to process these DEM files and provide maps of the watershed, stream order, stream flow, flow direction, and flow accumulation. These were produced to provide input for the methodology framework depicted in figure 5 below. Table 2 lists the information needed for this investigation.

Table 2: Required data and their sources.

Data	Parameter	Data type variable	Level of meacurement	Source
Cloud free and radiometrically corrected Level 2 multi-temporal satellite imageries (Thematic Mapper (TM), Enhanced Thematic Mapper Plus (ETM+))	Land use/land cover type	Qualitative	Nominal	USGS
DEM	Slope, elevation, flow direction	Quantitaive	Ratio	USGS
Soil	Soil type	Qualitative	Nominal	DSM
Distance to river	River buffer	Quantitaive	Ratio	DSM

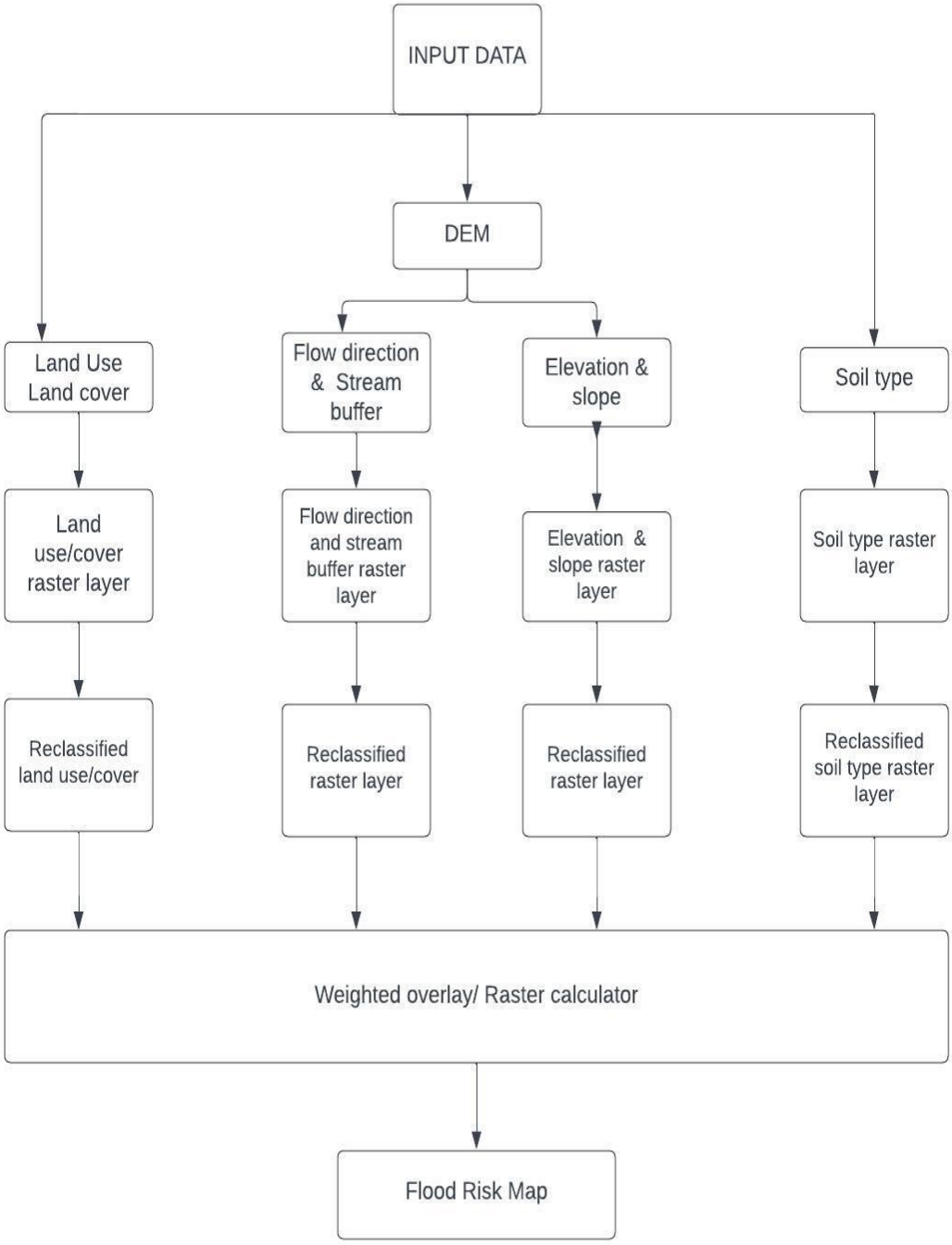


Figure 3: Methodology flow chart

3.2.2 Land Use-Land Cover Classification

The initial phase of image classification involved devising a classification scheme for land use and land cover categories within the study area. This process entailed selecting which land use and land cover classes to incorporate, aided by a familiarity with the local environment and previous research conducted in the area. Given the variability in climatic, economic, and social conditions across different regions, there are no universally agreed-upon definitions for land cover classes (FAO, 2016). The descriptions of these classes were derived from assessments conducted in Botswana and previous studies on land use and land cover in the Makgadikgadi pans region.

The process of image classification involves several key steps. Initially, spectral bands from multi-temporal satellite images are stacked and integrated into software like ArcGIS pro. These composite Landsat images are then corrected for geometry and registered to the UTM WGS 1984 projection system. False-color composite band combinations are applied to enhance the visualisation of the Landsat images (Keagakae, 2020). For the selection of validation samples, 150 sampling points are distributed across three study periods. Sampling points from historical periods are randomly chosen and adjusted to ensure equitable distribution and accuracy. This number allows for adequate representation of different flood scenarios while minimizing potential biases in data collection. According to research, a sample size of around 100-200 points is often recommended for achieving reliable results in flood risk assessments (Madzudzo et al., 2018). These sampling points are physically collected in the field using Garmin handheld GPS devices.

The image classification process in this study utilises the maximum likelihood classification algorithm, known for its perceived accuracy in assigning pixels to different land

classes (Lambin, 2003). This algorithm operates based on the probabilities of pixels belonging to specific land cover categories and is commonly employed for analysing Landsat surface reflectance images (Lambin, 2003).

An error matrix that cross-tabulates the land cover classes was created to verify the classification and determine the accuracy of the user, producer, and overall classification (Lillesand et al. 2014; FAO, 2016). On the other hand, the error matrix shows how effectively the statistics taken from the sampled classes can be applied to classify the same classes. It doesn't reveal the classifier's performance in other areas of the picture (Lillesand et al. 2004). In order to get over these restrictions, the Kappa Coefficient was used to calculate an adjusted measure of agreement for chance agreement between the field data and the classification findings (Lillesand et al. 2014; Elias et al., 2018). It was determined that the Kappa coefficient was:

$$K = \frac{\sum_{i=1}^{r} X\,ii - \sum_{i=1}^{r} (x_{i+} * x_{+i})}{N^2 - \sum_{i=1}^{r} (x_{i+1} * x_{+i})}$$

where **N**, which in this case consisted of the land cover classes for both classification data and field data for the 2020 image, is the total number of observed pixels in the matrix.

The land cover classes from the classified data in this study made up the number of rows, or **r**, in the error matrix.

The number of sites in row I and column I, denoted as **Xii** in this study, is made up of land cover classes that were accurately categorized and confirmed during the field survey.

The total number of sites in column I, denoted as **x+i** in this study, was made up of all the land cover classes that were obtained from the field survey.

According to Elias et al. (2018), a value of more than 0.80 indicates good classification, meaning that there is a higher degree of agreement between the classification and field data than would occur by chance; a value between 0.40 and 0.80 indicates moderate classification results, and a value less than 0.40 indicates poor classification. Consequently, the study's overall accuracy and kappa coefficient were 85.33% and 0.721, respectively. This indicates that moderate classification accuracy was established based on the Kappa value (Elias et al., 2018) (Table 3).

Table 3: Accuracy Assessment for 2020 OLI Image Analysis

Land Cover Land Use Class	Reference Totals	Classified Totals	Number Correct	Producers Accuracy	Users Accuracy
Water	30	30	30	100%	100%
Settlement	30	35	27	90%	77%
Bareland	30	38	30	100%	78.9%
Shrubland	30	20	18	60%	90%
Trees	30	27	23	76.7%	85%
Total	**150**	**150**	**128**		

Overall Classification Accuracy = 85.33%; Overall Kappa Statistics = 0.721

OA, PA, UA and K are computed as below:

$$\text{Overall Accuracy} = \frac{Sum\ of\ diagonal\ tallied\ (correctly\ identified)}{total\ number\ of\ samples} \times 100$$

$$\text{User's Accuracy} = \frac{Samples\ correctly\ identified\ in\ the\ row}{Row\ total} \times 100$$

$$\text{Producer's Accuracy} = \frac{Samples\ correctly\ identified\ in\ the\ column}{Column\ total} \times 100$$

$$\text{Kappa coefficient } (\widehat{K}) = \frac{Observed\ accuracy\ (P_0) - Chance\ agreement\ \ (P_e)}{1 - Chance\ agreement\ \ (P_e)} \times 100$$

3.2.3 Data analysis

3.2.3.1 Objective one (Gumbel distribution)

The amount and frequency of floods were ascertained by performing a magnitude and frequency study of the total yearly rainfall. Reappearance periods (R.I. or T) and exceedance likelihood were calculated using Gumbel distribution (Bhagat, 2017) in Microsoft Excel, and the results were summarised into magnitude-frequency curves for the Nata rain gauge station.

$$T = \frac{n + 1}{m}$$

where **T** is the recurrence interval in years, **n** is the number of record years, and **m** is the flood rank. With one being the highest.

The sorted data and interval data, which were calculated using the provided formula, were organized into tables and included in the appendices. This data will be used to create graphs showing the total rainfall, as well as the magnitude and frequency.

3.2.3.1.2 Validating Gumbel Distribution

When assessing flood data, there are numerous techniques to validate the Gumbel distribution method:

• **Comparison with past flood data:** Analysing the estimated flood frequencies and magnitudes against past flood data from the area of interest is one way to verify the methodology. A strong correlation between the actual and estimated values suggests that the Gumbel distribution is a suitable tool for examining the flood data.

• **Sensitivity analysis:** Analysing how sensitive the estimated flood frequencies and magnitudes are to changes in the input data is another way to verify the procedure's dependability. For example, by choosing arbitrary subsets of the input data and seeing if the estimated levels of flooding stay constant. The Gumbel distribution is a dependable technique for flood data analysis if the predicted values exhibit little variance across various data subsets.

• **Comparison with alternative methods:** Lastly, additional validation of the Gumbel distribution methodology may be obtained by contrasting it with other techniques like the Weibull distribution and the Log-Pearson Type III distribution. The Gumbel distribution's use as a practical technique for flood data analysis would be further supported if it showed improved performance in properly predicting flood frequency and magnitudes.

3.2.3.2 Multi criteria analysis

Applications for GIS and remote sensing were used to analyse spatial data. ArcGIS Pro was utilised for image processing, mapping, and analysis based on how each aspect improved the

data analysis. In addition to being utilised to retrieve photographs, Google Earth was also employed for analysis aimed at validating satellite imagery (Samuel, 2021). The weights of the attributes utilised for the weighted overlay analysis in the flood risk mapping were determined using multi-criteria evaluation (Figure 5). Expert judgement and the percentage of land linked with risk were used to compare and weigh the characteristics.

The criteria being utilised for the weighted overlay procedure require spatial data. Elevation, Slope, Stream buffer, Soil Type, Flow Accumulation, and Land Use/land Cover are the requirements. Maps were created for every parameter using ArcGIS's reclassification tool. STRM DEM is used to create raster maps for elevation, slope, and drainage. Surface interpolation is used to convert precipitation data into a raster map. An image from Landsat 9 is used to construct a polygon map for land cover, and a paper map is used to digitise a polygon map for soil type.

3.2.3.2.1 Flow accumulation

The DEM is used to create the stream network. The conceptual overview for this stage is shown in Figure 6. Because a DEM without depressions is necessary for watershed delineation, sinks in the DEM are found using the sink tool in ArcGIS hydrology, and then they are filled in using the fill tool. Next, the flow direction tool is used to establish the course in which water current will take, and the flow accumulation tool is used to compute the number of cells that would flow into each filled DEM cell. The areas draining to certain spots on the DEM can be identified using the Flow Accumulation grid. The entire map's watersheds are then created using the Basin tool, which is used to detect basin pour points and generate watersheds.

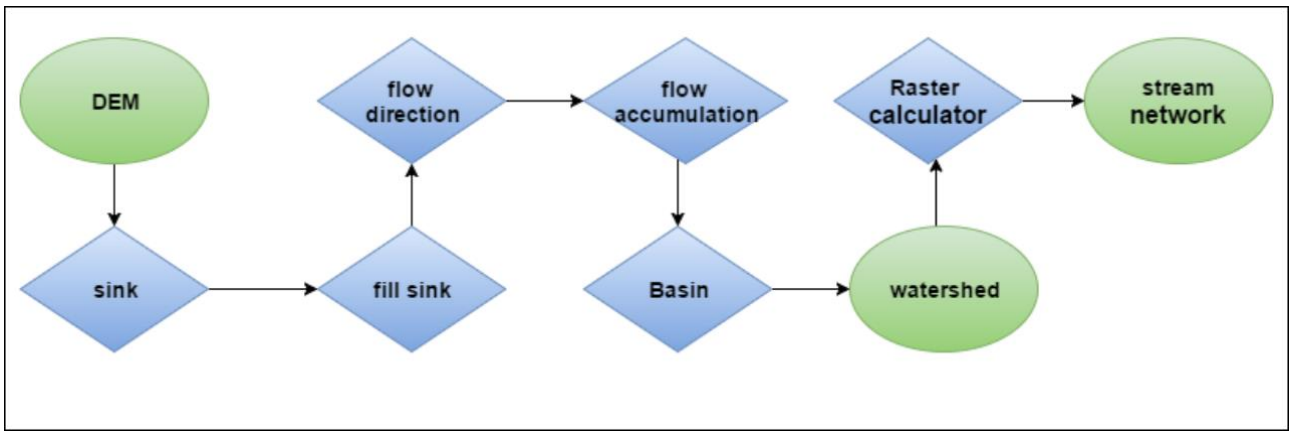


Figure 6: Flow chart for watershed and stream network delineation

A provisional argument is directed to the flow accumulation raster in order to determine the stream network. The plan is to reclassify all cells as no data and all other cells as 1 when they hit a specific accumulated flow threshold. Since 900 will be the threshold utilised in this analysis, any cells with values higher than 900 will be categorised as 1. The Nata basin's drainage was thought to be best represented by the threshold of 900.

3.2.3.2.2 Elevation and slope

The ArcGIS spatial analyst toolbar's surface analysis tools are used to determine the elevation and slope from the DEM. Slope and elevation maps are created by using the contours of the research region that were extracted from the DEM. A certain area's flow and flooding are impacted by the slope's steepness. In comparison to places with steep slope angles, low-lying areas with gentle slope angles typically experience floods earlier. Flat terrain reduces water runoff, which leads to significant penetration in areas with open soil or stagnation in areas with impermeable surfaces, both of which result in water logging conditions.

Five classes are identified on the slope map using the Natural Breaks (Jenks) distribution. Since the Natural Breaks (Jenks) distribution can identify true classifications in the data and produce choropleth maps that accurately represent data patterns, it is utilised to classify the elevation map into five groups. Following that, these categories are arranged according to the preset rankings.

3.2.3.2.3 Land use/land cover

The LULC map that was created had five features: buildup area, flora, water, woodland, and bare plain. After that, a fresh categorisation is used for the overlay study. The built-up area land cover is ranked as "very high" because of its high impermeable surface, making it the most vulnerable to flooding. Vegetation and bare ground land covers are among the next highest land covers most vulnerable to flood because of their compressed structure. The coverage of forest land and water are ranked as poor and moderate, respectively as seen on table 4.

Table 4: Land cover ranking

Land use/cover	Ranking
Trees	Low
Water	Moderate
Built up area	Very High
Grass	Moderate
Ground	High

3.2.3.2.4 Geology (soil type)

In the ArcGIS pro-environment, the soil file was imported as a polygon shapefile. The research region was then removed, and the polygon shapefile was projected to UTM Zone 35S and georeferenced to the WGS 84 geographic coordinate system. Right-clicking on the soil shapefile in the table of contents in ArcMap allowed the user to pick "Properties," then "Symbology," change the "Value field" to "SNUM," click "Add all values," and then click OK to confirm. The user went to Arc Toolbox, clicked "Conversion tools," then "To Raster," selected "Polygon to Raster," and entered the polygon shapefile into the dialogue box to produce the final soil map in raster format.

The dominating soils in the study area are Arenosols, Sandy soils, and Fluvisols. Arenosols make up 58% of the basin and are characterised by low permeability, leading to a higher flood hazard. Sandy soils, with their high infiltration rate, are less prone to flooding, although areas with high erosion potential may still face flash flood risks. Fluvisols, covering 41.9% of the basin, are rich in clay and have low infiltration capacity, making them highly susceptible to flooding, particularly in the southern region near the pan.

3.2.4 Analytic Hierarchy Process (AHP)

An organised method for making decisions is known as multi-criteria analysis. MCA refers to any intentional and methodical process used to identify general preferences among available options with the goal of ranking them from most to least significant. A collection of weights for the many choices is what MCA produces. Choosing By Advantages (CBA), Aggregated Indices Randomisation Method (AIRM), Characteristic Objects Method (COMET),

Analytic Network Process (ANP), Analytic Hierarchy Process (AHP), Best Worst Method (BWM), etc. are a few examples of MCA techniques. Based on research, this dissertation utilises the Analytic Hierarchy Process (AHP) method as it is the most commonly utilised method for flood analysis. A decision problem can be broken down into a hierarchy consisting of criteria, alternatives, and aim.

Creating a flood danger map is the aim of this thesis, and the parameters that will be employed include drainage, elevation, precipitation, soil type, land cover, and slope. This is predicated on comparing the criteria in pairs. Next, the choice criteria's priorities are estimated. Due to the fact that the pairwise comparison matrix converts subjective priorities based on the preferences of decision makers into numerical values, it is crucial. Figure 7 illustrates the procedure. The process is demonstrated in figure 7.

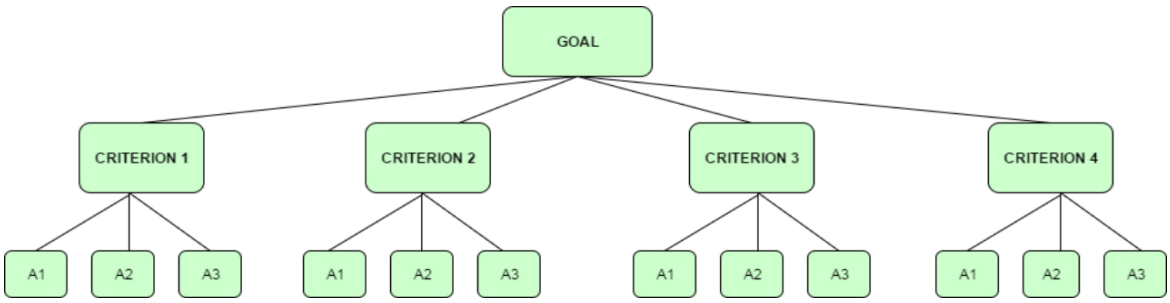


Figure 7: The AHP process

3.2.5 Pairwise comparison method

The factors that have been found to influence floods in the study area are used as analytical criteria in this thesis. Based on the following components, a matrix is created for the chosen criteria:

C1: Slope

C2: River buffer

C3: Soil type

C4: Elevation

C5: Flow accumulation

C6: land use land cover

The decision-maker compares each criterion to the others in a pairwise comparison matrix in order to ascertain which of the two criteria has a greater chance of having an impact on local flooding. If criteria A and B have equal weight, the pair is assigned an index of 1.The pair is given an index between 2 and 9 if criteria A is more influential than criteria B. Higher numbers denote greater influence. The reciprocal of this index is used in the inverse evaluation. The matrix is normalised to make sure that each column sums up to one when the pairwise comparisons are finished. Divide each element in each column by the total of those columns to arrive at this. The criteria weights {W} or priority vector are then found by taking the average of the values for each row.

3.2.6 The weighted overlay process

There are three important steps involved in the weighted overlay process. Each raster layer is initially assigned a percentage weight (the criteria weights determined in the AHP) to highlight the relative importance of each layer in the analysis. The values within each raster layer are ranked second (using an appropriateness scale) to compare the different types of information present in each raster layer. Lastly, all the raster layers utilised in the analysis are overlaid. Each

raster cell's ranking value is multiplied by the weight of the layer it is on before being added to the ranking assessments of the raster cells it overlays. Every criterion that was taken into consideration was rated in the order of preference during the ranking step.

Most important = 1, least important = 9, and vice versa, are the two common ways to rank things. The other is inverse ranking, which says most important = 9. The classification used in this investigation is based on the degree of flooding, with high being ranked at 1, moderate at 2, low at 3.

For the analysis, the spatial analyst's weighted overly tool is used. The pairwise comparison weights are used to weight the six reclassified raster layers, which are then combined according to the provided rankings. After multiplying each input raster's cell values by the raster weight, the final output raster is produced by putting them all together. The output raster is a flood danger map that shows which places are susceptible to the various levels of flooding described above.

3.3 Flood extent (Objective 3)

By contrasting the mapping results with actual flood occurrences that have happened in the past, the flood risk mapping method can be made valid. By contrasting the model's anticipated flood risk with the actual flood extent, the validation may be carried out. Statistical metrics like sensitivity, specificity, and accuracy can be used to evaluate the model's accuracy. In the case for this study flood extent will be determined from satellite images and the produced flood extent map will be compared to the flood risk map produced to test its validity. The flood extent map was produced following the process in figure 8.



Figure 8: The water cover extent process

1.**Load the satellite imagery:** Open ArcGIS Pro and load the satellite imagery of the area of interest.

2.**Preprocess the imagery:** Preprocess the imagery to correct any distortions, enhance the image quality, and remove any artifacts that could affect the NDWI calculation. The researcher used the Image Analysis window in ArcGIS Pro to perform radiometric and atmospheric corrections. Radiometric correction was performed to adjust the pixel values to account for sensor errors and inconsistencies, ensuring that the reflectance values accurately represent the Earth's surface. Atmospheric correction was applied to eliminate the influence of atmospheric particles (such as water vapor, dust, and aerosols) that can scatter and absorb light, thereby distorting the spectral values. These corrections were necessary to enhance the image quality and ensure the NDWI results are consistent and precise for identifying water bodies.

3.**Calculate the NDWI:** By deducting the near-infrared (NIR) band reflectance from the green band reflectance and dividing the result by the sum of the two reflectance, one may compute the NDWI for an image using the Raster Calculator tool in ArcGIS Pro.

4.**Set a threshold:** Using ArcGIS Pro's Histogram tool, set a threshold to differentiate between pixels that contain and do not contain water. The thresholds used in this study to differentiate between pixels containing water and those that do not were determined based on the NDWI

values. Typically, NDWI values greater than 0 indicate water bodies, while values less than 0 represent non-water features such as vegetation, soil, and built-up areas.

5.**Generate a binary image:** Create a binary image by using the Raster Calculator tool to classify all pixels with an NDWI value above the threshold as water, and all pixels with an NDWI value below the threshold as non-water.

6.**Create a flood extent map:** Overlay the binary water mask onto a map of the River basin to create a flood extent map.

Secondly different scenarios will be created based on the weights given to the criterions to determine the sensitivity of the method used for the overlays. For Sensitivity analysis, it will be carried out to offer more useful insights for enhancing the model's capacity to produce more practical results (Samuel, 2021). The flood risk maps for scenarios S1 (the original flood risk map), S2, and S3 will be compared to the original flood risk map developed in this study, which is believed to be the most reliable scenario, as there were no prior flood risk maps in the research area to validate the flood risk maps generated.

The following presumptions will serve as a guide for developing scenarios:

I. The first scenario assumes that land use and stream buffer generate higher risk, and
II. The second scenario assumes that land use and Elevation produce higher risk.
III. The final scenario assumes that Stream buffer and elevation present the highest flood risk.

Chapter 4

RESULTS AND ANALYSIS

4.1 Flood frequencies and occurrences

Finding the size and frequency of floods is the study aim (a) under which the data are given. In doing so, the chance of occurrence, and the magnitude and occurrence analysis of the total precipitation for the linked floods were all considered. The kind of data consists of monthly rainfall depth (mm) records; for analysis, the highest monthly values were utilised. The Gumbel distribution's position and scale parameters are found in Table 5, where columns present the mean and standard deviation of the rainfall data.

Mean (158.2035484): Represents the average annual rainfall calculated from the dataset.

Standard Deviation (64.06770848): Indicates the variability or dispersion of the rainfall data.

Ym (0.5362): This is the reduced mean of the Gumbel distribution, which depends on the sample size and is used in the calculation of rainfall extremes.

Sm (1.1124): This is the reduced standard deviation in the Gumbel distribution and aids in defining the spread of the data.

N	31 years
Mean	158.2035484
Std.Dev	64.06770848
Ym	0.5362
Sm	1.1124

Table 5: Table showing variables used in Gumbel distribution M

4.1.1 Flood frequency analysis

This study assessed the patterns of flooding at a rainfall station in Nata. Figure 9 shows the expected amount and frequency of rainfall events at the site based on yearly maximum rainfall data from 1991 to 2021, a 31-year period. According to the precipitation magnitude-frequency curve, there is a 100% chance that annual precipitation of 300.59 mm will occur every 32 years, while annual precipitation of 63.28 mm is most likely to occur every year. Large rainfall events usually have low incidence rates but long return intervals or high recurrence rates. The trend line equation demonstrates that the pattern scatter and R^2 value, which are both 0.9618, are narrow and appropriate for forecasting the maximum monthly rainfall expected in the Nata river basin.

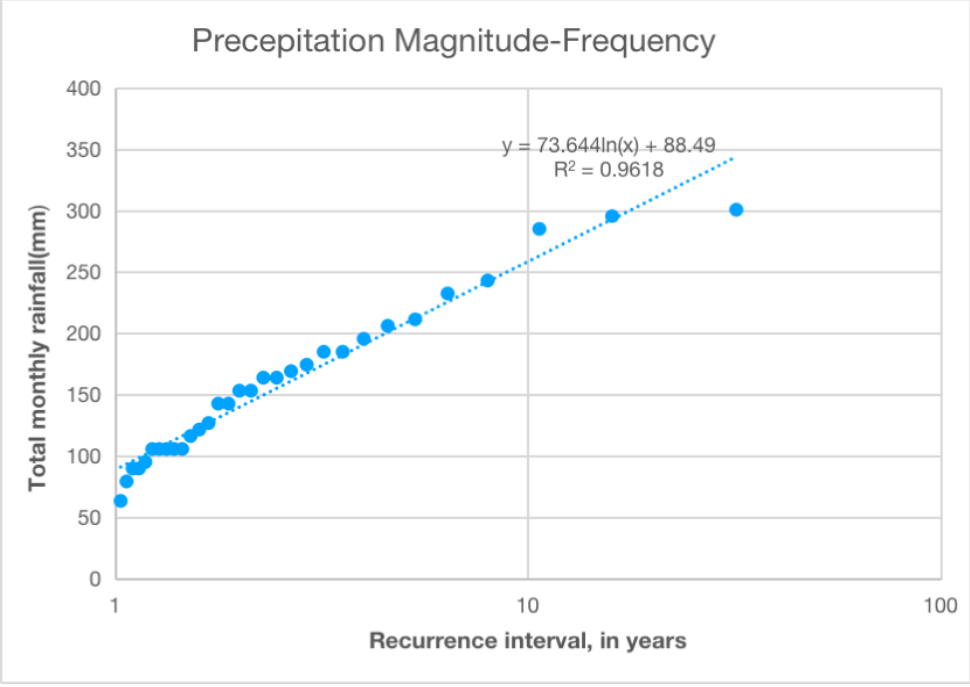


Figure 9: Total rainfall magnitude-frequency graph for Nata

4.1.2 Probability of occurrence

The deduced tendencies for the likelihood of floods at the Nata rainfall station are shown in this section. Figure 10 shows the station's graphs. The graph indicates that there is a 3% chance of 301 mm of rainfall. There are greater odds of having 63mm, as indicated by the lower percentage exceedance likelihood of 97%. These findings demonstrate that while smaller rainfalls have a higher chance of occurring, higher rainfalls have a lower probability of occurring.

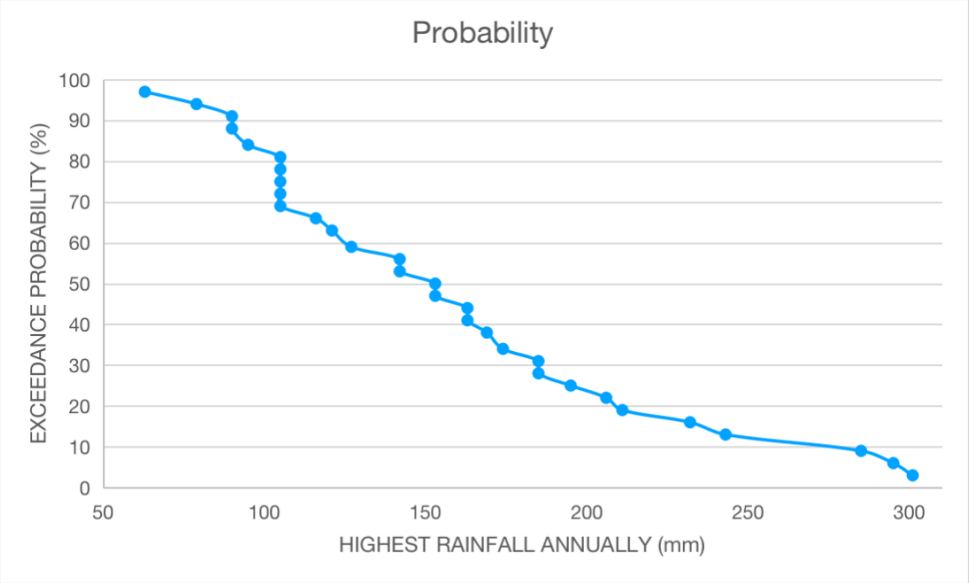


Figure 10: Graph showing the probability of rainfall occurrence.

In order to verify the amount and frequency of floods in Botswana as a whole, Table 6 provides historical data from Botswana statistics, consist of the dates when floods happened in Botswana, the amount of precipitation, and the documented cost. The data in Table 6 clearly demonstrates that in 2000, the highest monthly total rainfall of 242.58 mm resulted in floods that had a negative impact on the country's economy. Rainfall in the years that followed (2001–2017)

was less than in 2000, yet it still resulted in significant damage and a high number of fatalities. The most recent floods in 2017 brought on by cyclonic effects also had the greatest monthly rainfall total (184.57mm), and the destruction significantly increased economic loss.

The table 6 includes rainfall information together with Gumbel distribution methods for calculating flood magnitude and frequency estimates. The rainfall data indicates the highest annual rainfall that has been observed in a certain area during a specific time period. The Gumbel distribution formulas are used to estimate the size and frequency of floods with various return periods and to fit a probability distribution to the rainfall data.

Table 6 : Computation Table of Gumbel's Extreme Value Distribution Method

YEAR	Precepitation	Rank(m)	P=m/(N+1)	T=1/P
1997	300.59	1	0.03125	32
2018	295.31	2	0.0625	16
2008	284.77	3	0.09375	10.66666667
2000	242.58	4	0.125	8
2009	232.03	5	0.15625	6.4
2011	210.94	6	0.1875	5.333333333
2001	205.66	7	0.21875	4.571428571
2021	195.12	8	0.25	4
1996	184.57	9	0.28125	3.555555556
2017	184.57	10	0.3125	3.2
2020	174.02	11	0.34375	2.909090909
2013	168.75	12	0.375	2.666666667
1998	163.48	13	0.40625	2.461538462
2007	163.48	14	0.4375	2.285714286
2014	152.93	15	0.46875	2.133333333
2016	152.93	16	0.5	2
2004	142.38	17	0.53125	1.882352941
2005	142.38	18	0.5625	1.777777778
2012	126.56	19	0.59375	1.684210526
1991	121.29	20	0.625	1.6
2002	116.02	21	0.65625	1.523809524
1993	105.47	22	0.6875	1.454545455
1994	105.47	23	0.71875	1.391304348
1999	105.47	24	0.75	1.333333333
2006	105.47	25	0.78125	1.28
2010	105.47	26	0.8125	1.230769231
1995	94.92	27	0.84375	1.185185185
1992	89.65	28	0.875	1.142857143
2003	89.65	29	0.90625	1.103448276
2015	79.1	30	0.9375	1.066666667
2019	63.28	31	0.96875	1.032258065

Method validation: The validation of the Gumbel distribution method using historical flood data provides evidence that the method is an appropriate way to estimate flood magnitudes and frequencies in the region of interest. This is important because it suggests that the method can be used to inform flood risk management strategies and to plan for future floods. The historical flood data can be seen in *table 7.*

Table 7 : Historical Floods Recorded in Botswana with the Rainfall Intensity and Damage Observed

Date	**The degree of precipitation Total monthly precipitation (mm)**	**Cost on the country**	**Sources**
1972 (January)	257.4	US$50 Economic Loss	(Samuel, 2021)
1988 (February)	254.4	8 Deaths; 12007 People affected	(Samuel, 2021)
1995 (March)	179.6	20 Deaths; 5500 People affected	(Samuel, 2021)
2000(February)	276.7	3 Deaths; 138276 People affected; US$2000 Economic Loss	(Samuel, 2021, IFRC, 2000)

2010 (January)	123.3	Data unavailable	
2012(December)	108	Data unavailable	
2013(December)	118.7	12 Deaths	(IFRC, 2013)
2015 (January)	80.6	Data unavailable	
2017 (February) Cyclone Dineo	170.8	650 Households affected; 500 Houses destroyed; Bridges collapsed; Roads closed	(Samuel, 2021)

4.2 Flood risk assessment with MCA

Results of the flood risk assessment through GIS and Remote sensing are interpreted in relation to the study objective number two, which is to provide standards for the geospatial flood disaster risk assessment. As seen below, this entailed creating the digital elevation model, hydrological indicators, land use/cover, topography/slope, and soil types.

4.2.1 Elevation and slope

According to Figure 11, the research region's catchment area is located between elevations of 806 and 1141 meters above sea level. The catchment area's southern and eastern edges have the highest elevations.

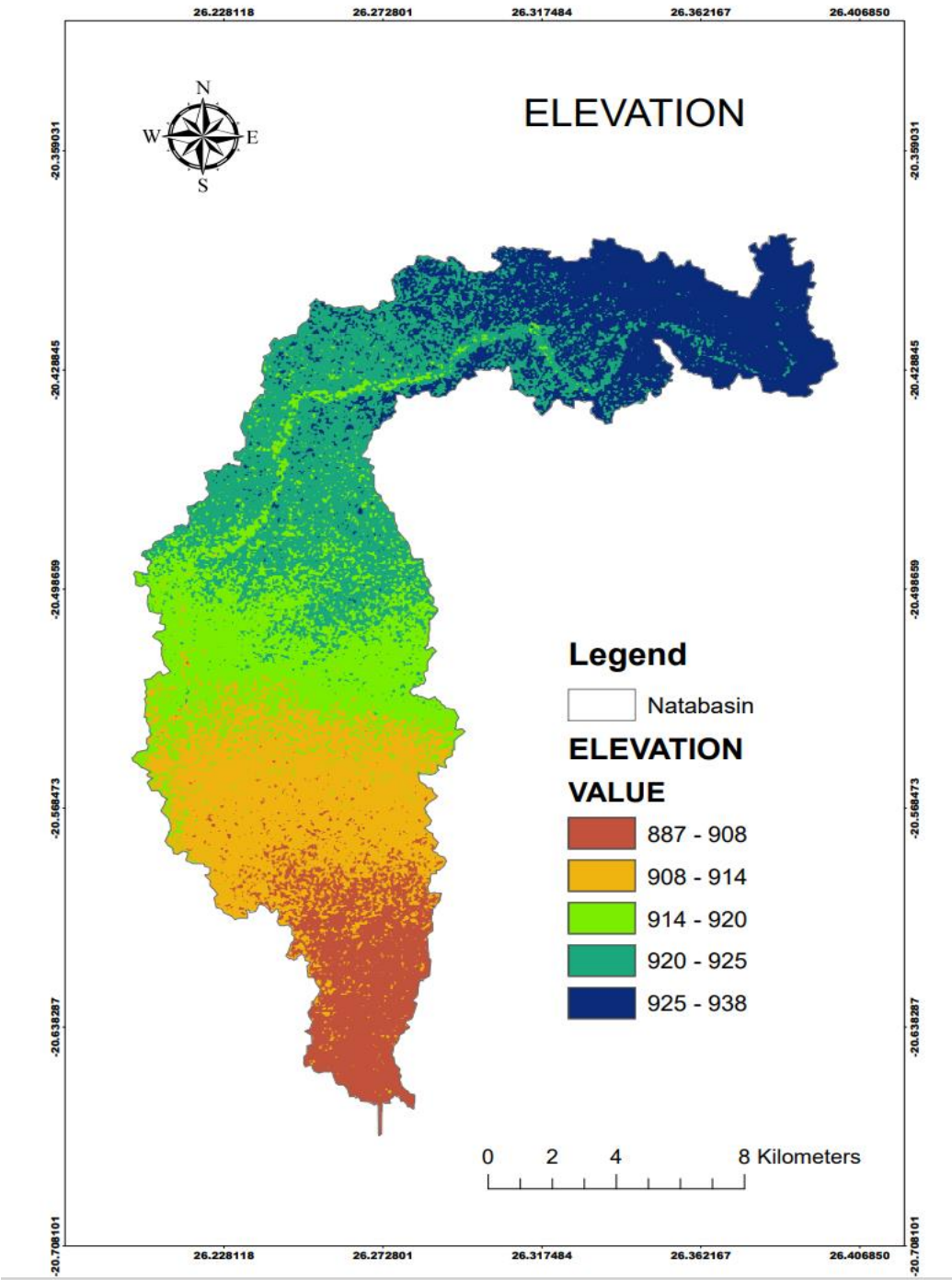


Figure 11: Elevation map for the study area

In the study area low lying land is found on the south just like in the main catchment area, but the study area has an elevation range of 887m to 938m above sea level. The study area has no major elevation defining features like hills or depressions. This can be deduced from the map

below, figure 12 showing the slope of the area. The highest point of the area can be seen on the northeastern side of the boundary, this study area has a gradual change in slope. The Natabasin boundary is outlined using a black line as shown in the legend. The white spaces outside this boundary represent areas that are not part of the Nata River Basin.

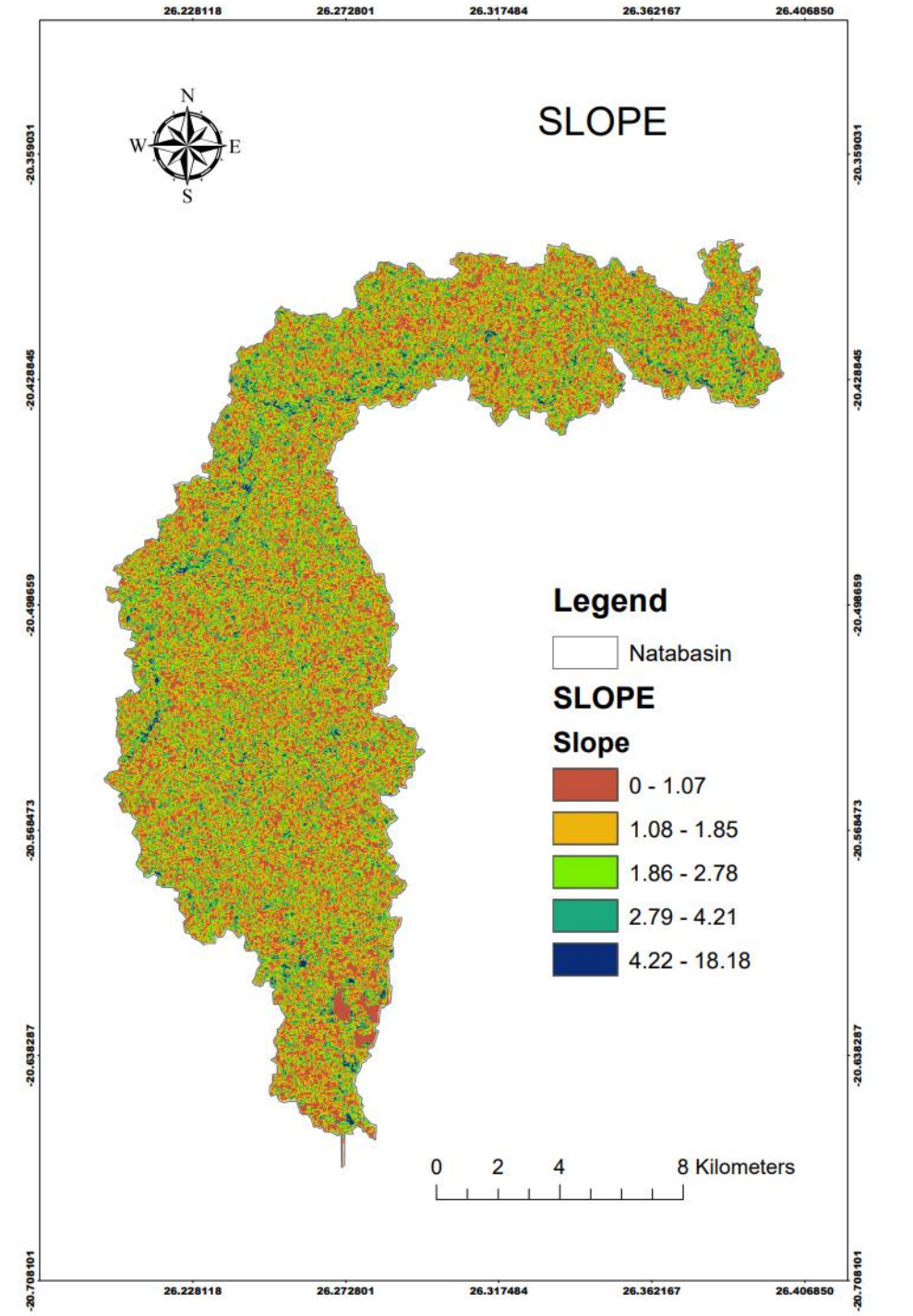


Figure 12: Slope map of study area

4.2.1.1 Reclassified slope and elevation

One of the most crucial factors in determining flood risk is elevation. Low-lying places are particularly vulnerable to flooding since even minor floods can cause them to be submerged (Ghosh & Kar, 2018; Ntajal et al., 2017). With decimal degrees and WGS84 datum, the United States Geological Service Shuttle Radar Topography Mission (SRTM) data (USGS) is the source of the Digital Elevation Model (30m) used to construct the elevation layer in the research region.

Important determinants of a terrain's vulnerability to flooding are its elevation and slope. The volume of surface runoff or subsurface drainage, infiltration, and flow direction are all impacted by slope. Because flat topography can result in stagnant water, low gradient slopes are especially vulnerable to floods. he research region is almost entirely flat, with minor natural undulations and irregularities defining the slope. Because the study region is flat, rainwater accumulates quickly, which leads to flooding. Figures 13 and 14 display the reclassifications.

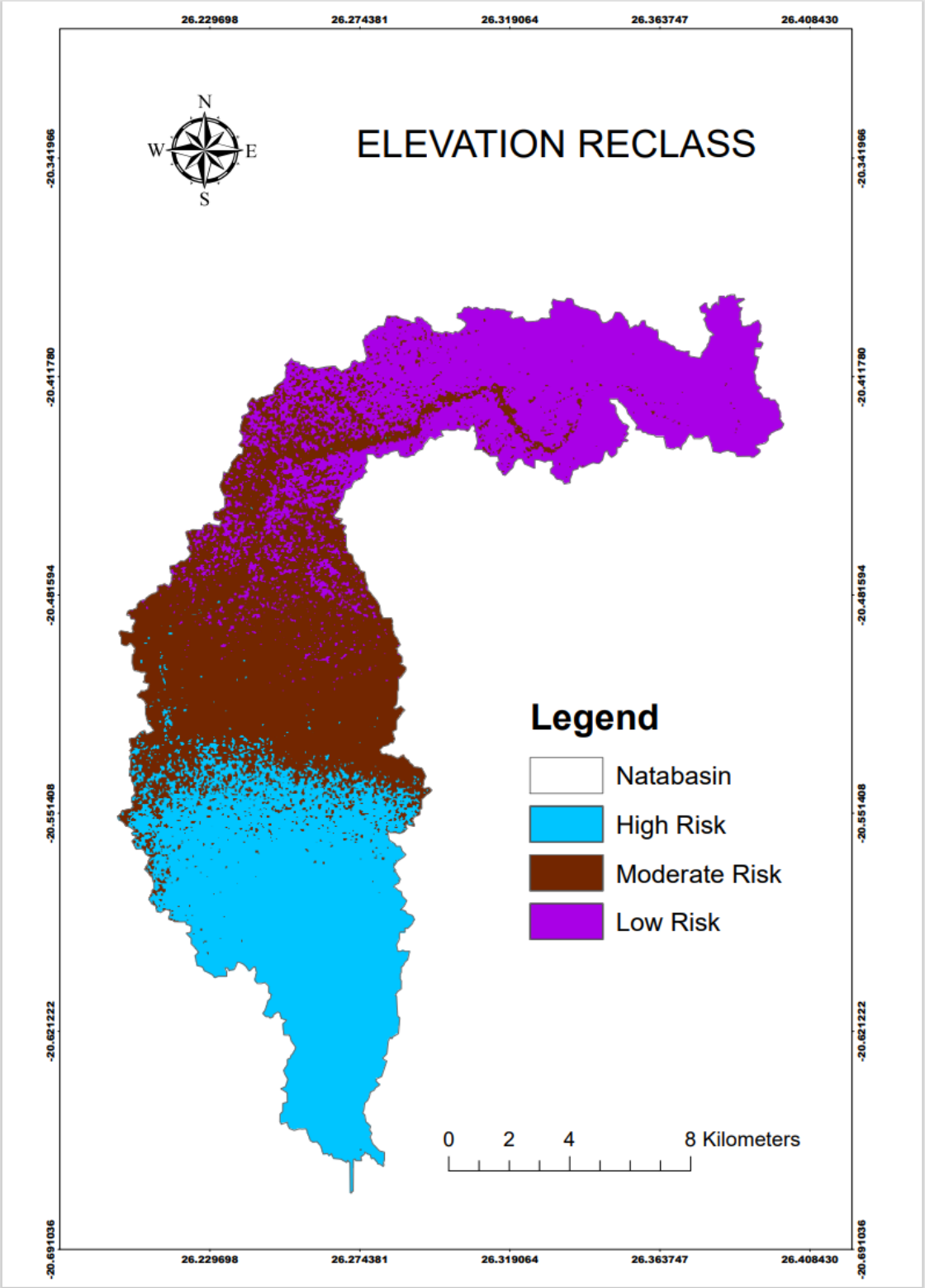


Figure 13: Reclassified Elevation of the study area

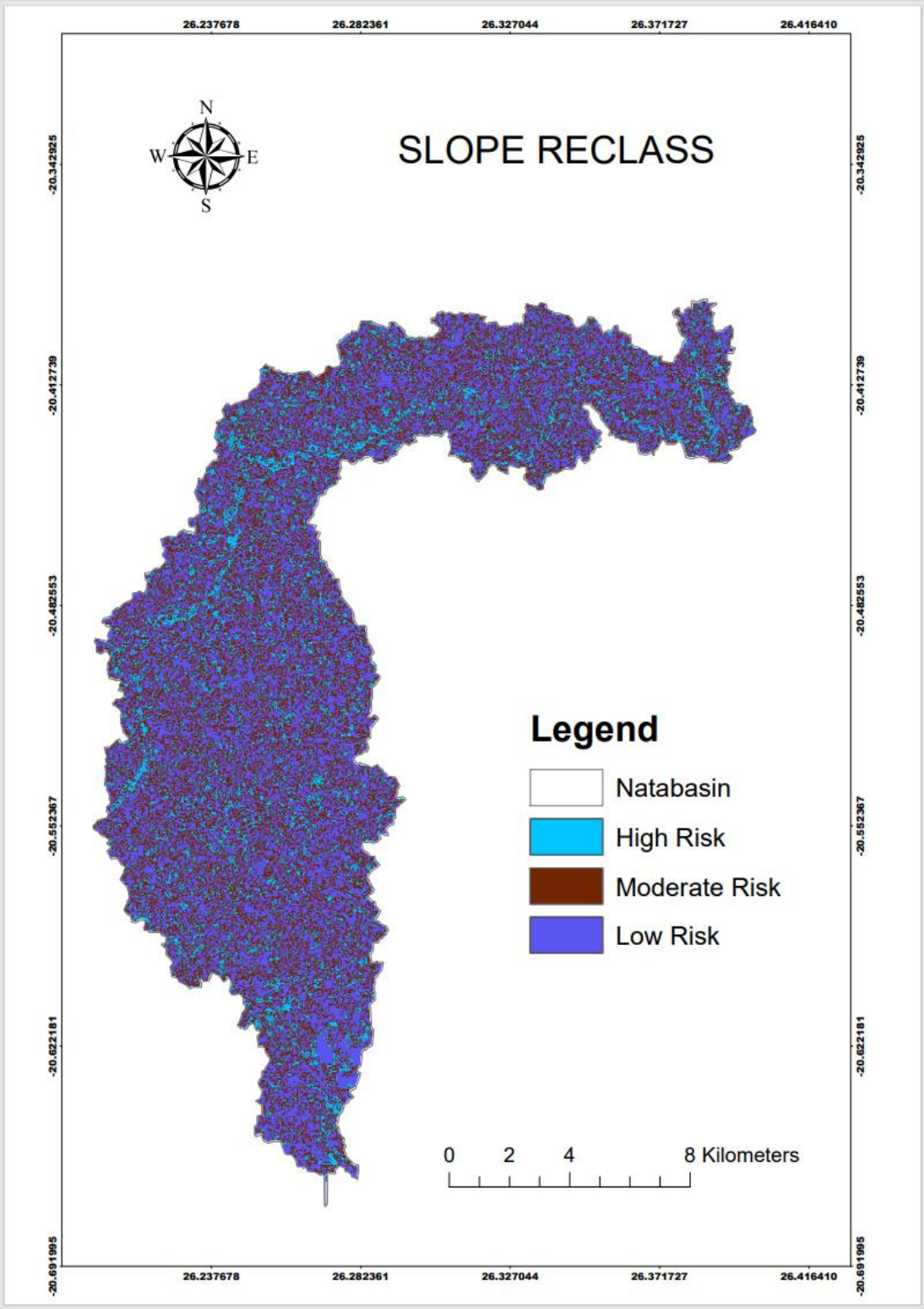


Figure 14: Slope map of study area

4.2.2 Hydrological indicators

This part evaluated and interpreted stream flow, flow direction, and flow accumulation to determine the degree of flood risk. These are covered in the section that follows.

4.2.2.1 Flow direction

The Nata River Basin research region, located in the Eastern Makgadikgadi watershed, has eight predominant directions of water flow, as depicted in Figure 15. There is no obvious direction to the water's flow because the ground is primarily level. It makes sense to direct flow to the south-eastern portion of the research area because there are greater red spots there, which are on the lower lying areas determined by slope and elevation. This increases the likelihood of flooding throughout the entire research area if the river and streams overflow.

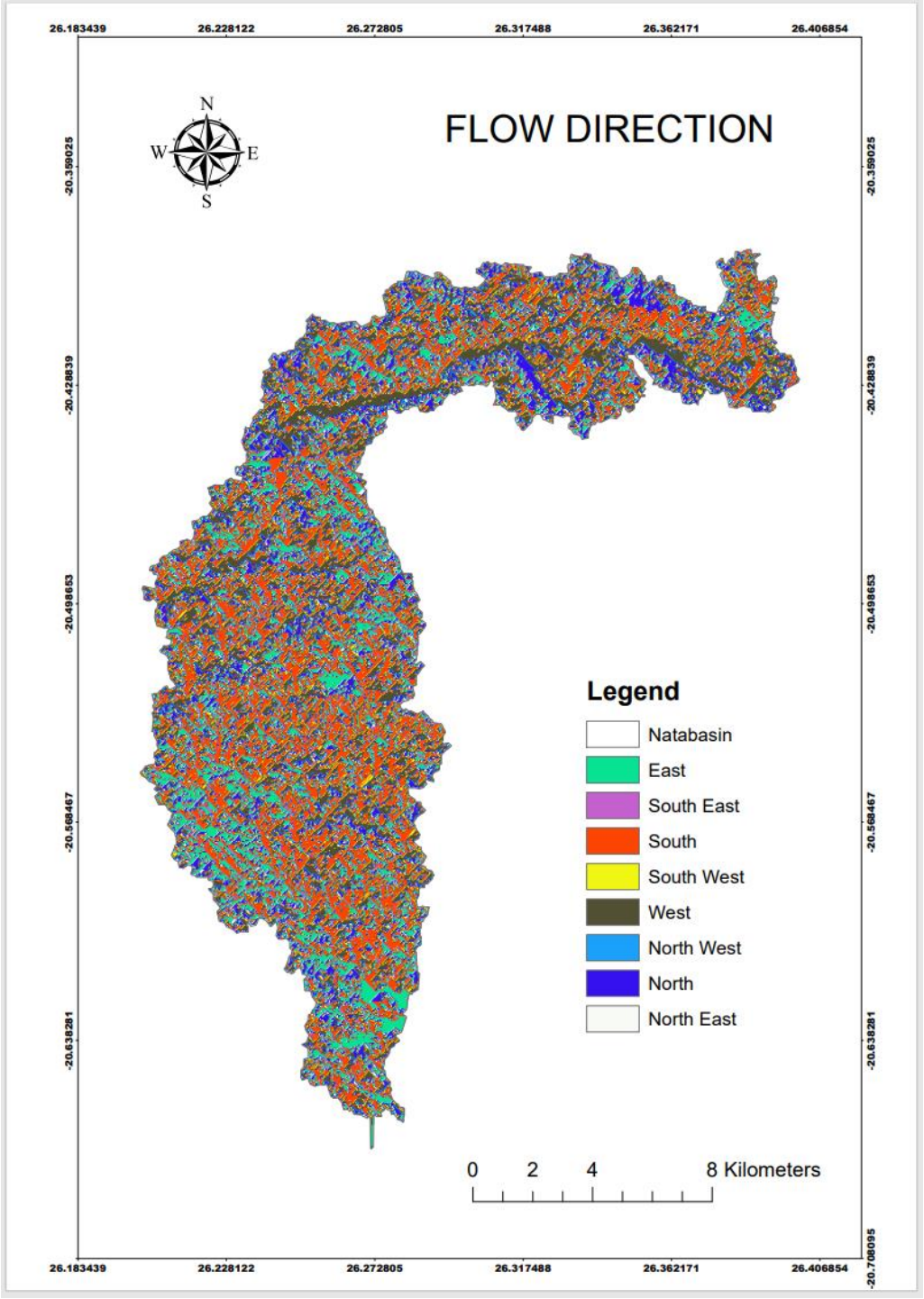


Figure 15: Flow direction in the study area

4.2.2.2 Streams

As depicted in Figure 16, three groups of streams were determined from the data in the Nata Basin. They range from lowest order streams which feed higher order streams, to highest order streams. Lower stream orders are linked to a higher risk of flooding. The settlement of Nata is on the first stream orders (Figure 16).

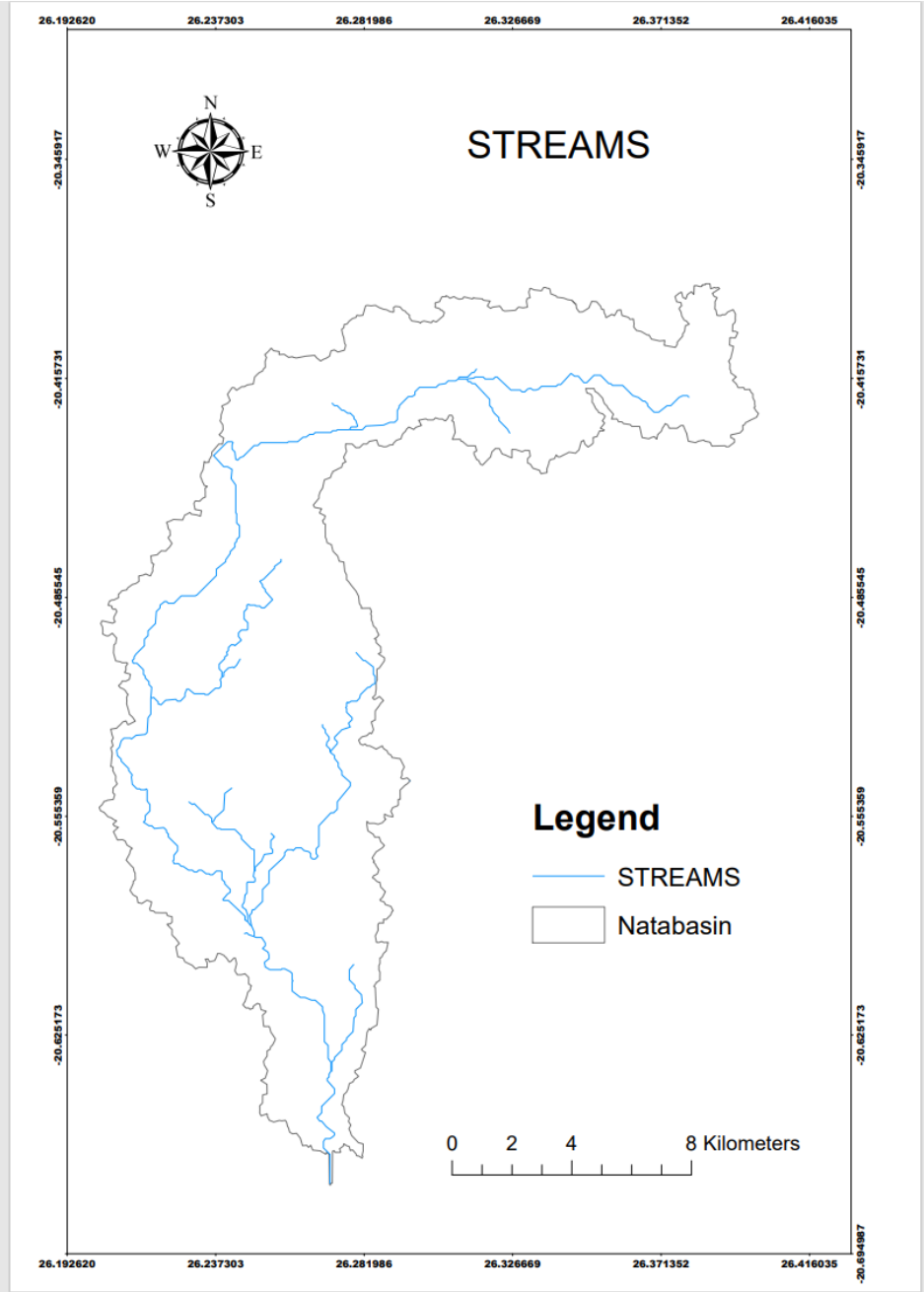


Figure 16: Stream order in the study area

4.2.2.3 Reclassified hydrologic indicators

With relation to stream buffer risks are higher in areas close to the river channels. Based on the historic flood records and expert judgement areas that are within 1000m from rivers are rated to have very high hazard of floods, whereas areas within distances of 1km, 2km, and 3km from rivers are considered to have high, moderate, and low flood hazard respectively. According to the probable influence of each hydrological element on flood risk, the hydrology map can be classed, with locations cover to river or high soil moisture being assessed as having a higher risk of flooding, the maps below (figure 17 and 18) show the re-classes.

.

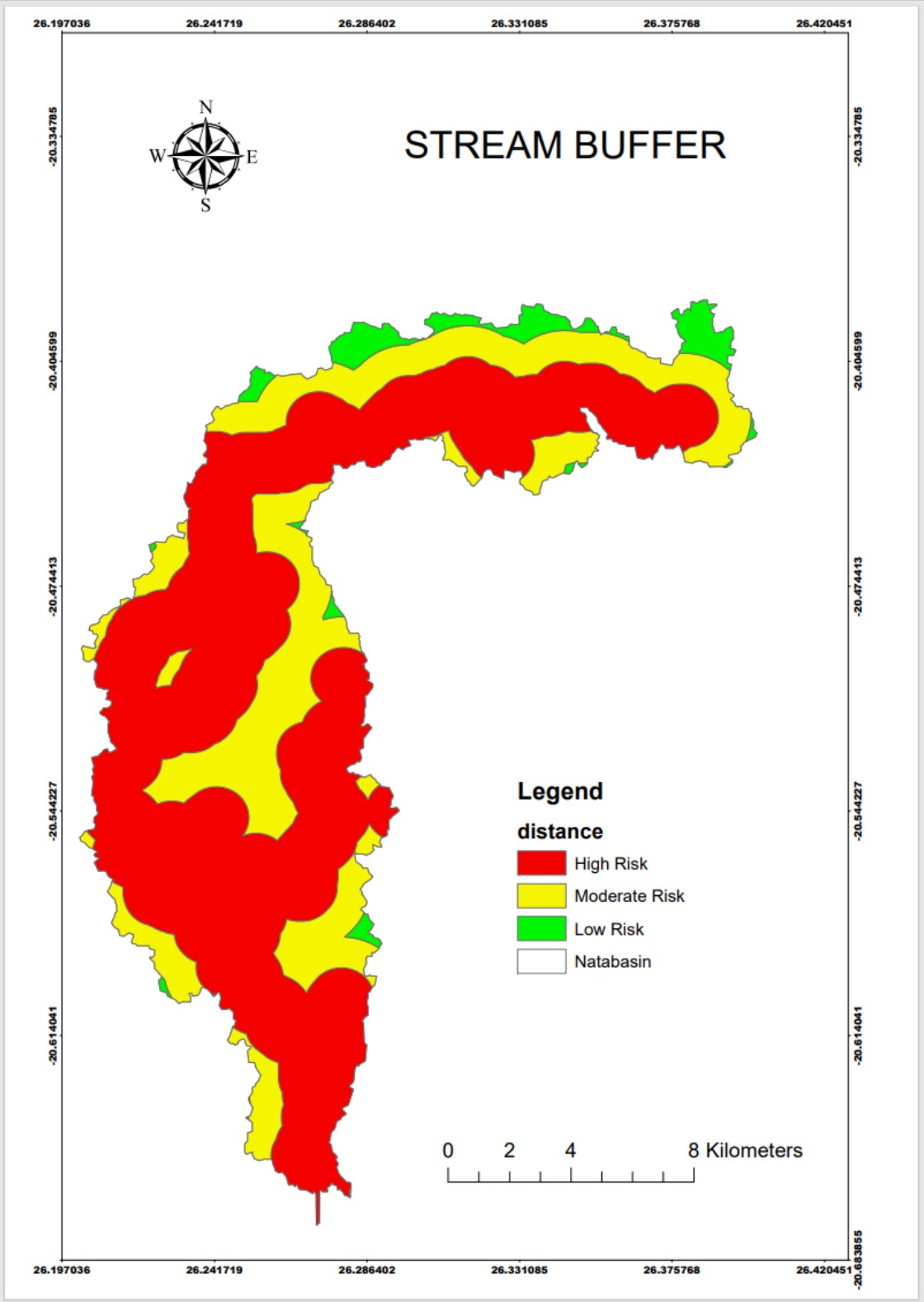


Figure 17: Stream Buffer for the study area

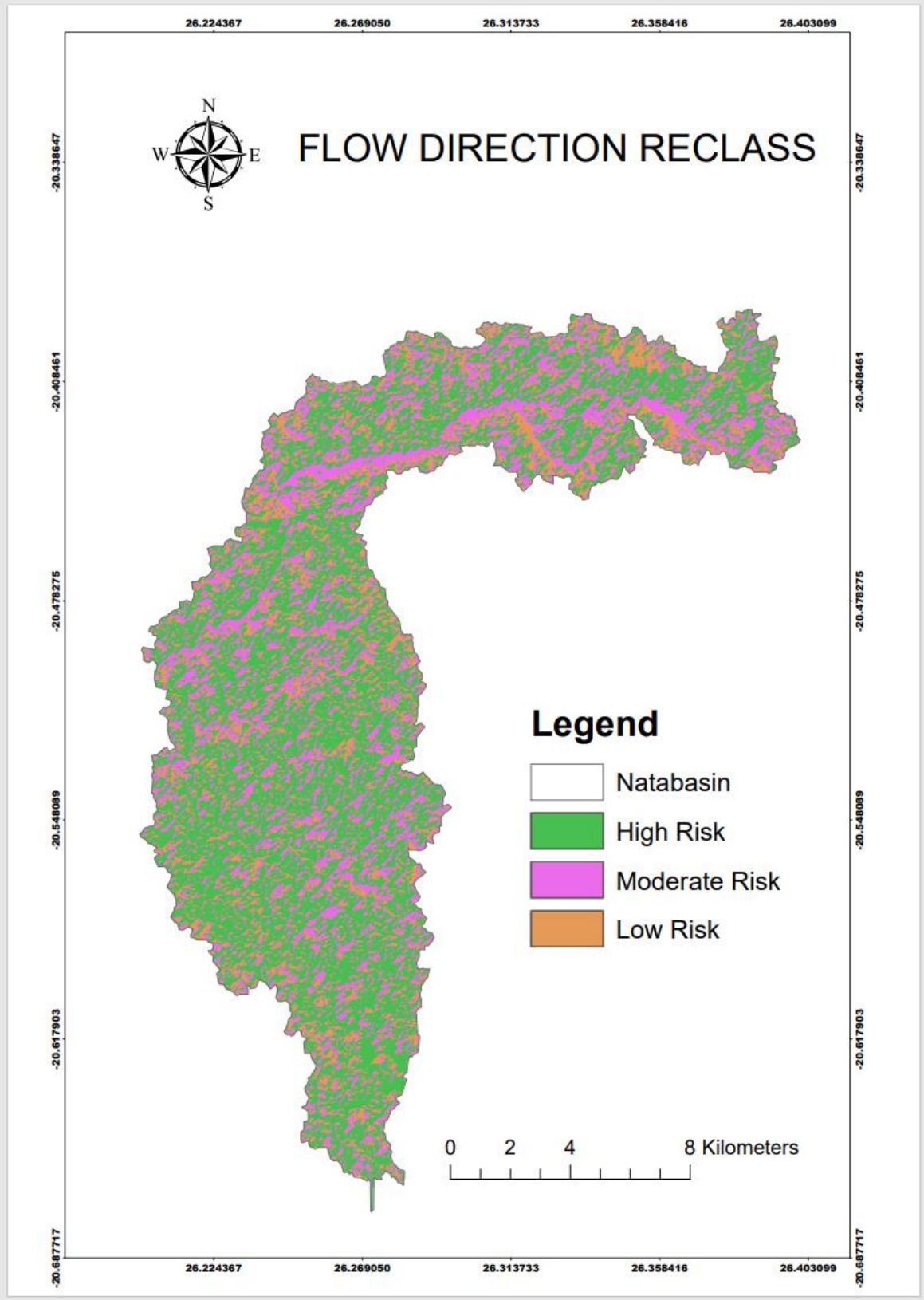


Figure 18: Reclassified flow direction for the study area

4.2.3 Land use land cover

~~The research area's land usefulness is shown via land use statistics. To create a risk map and send out early warnings to urban areas, which can help prevent disasters when large residential, commercial, and industrial buildings are situated in high-risk areas, land use data is necessary. To identify settlement land that is susceptible to floods as well as flood risk areas where there is a tree cover. In addition to this, hospital, school, and college building information can be extremely helpful during flood hazard in identifying building and structure locations as well as hydrologic parameters for a watershed. This data can be kept in a GIS database and used as needed in the future, hence the need for this criterion.~~

Figure 19 depicts the five broad land use cover classifications that make up the catchment region. Shrub land, tree-dominated land, barren territory, populated areas, and water bodies are some of these. These land cover types are uniformly dispersed throughout the basin. Because of the catchment's higher level of realised land cover diversity, each land cover will react and interact with surface runoff in a unique way. In contrast to the northern stream, where sparse shrubs and tree-dominated land are more common, the southern stream of the basin is dominated by bare-land and shrub-land (Figure 19). On the other hand, there is settlement areas at the center and sparsely south of the study area. As a result of possible planners' inability to follow adaptable construction rules, inadequate drainage, impermeable surfaces, and subpar agricultural methods, this also poses a risk of flooding. Large water features, including the Nata River, can be found as a land cover. As seen in Table 8 below.

Table 8 : Land cover distribution across the Nata Basin

Land Cover Type	Area (km2)
Water	1.87
Settlement	8.22
Shrubs	76.65
Trees	114.95
Bare-land	3.34

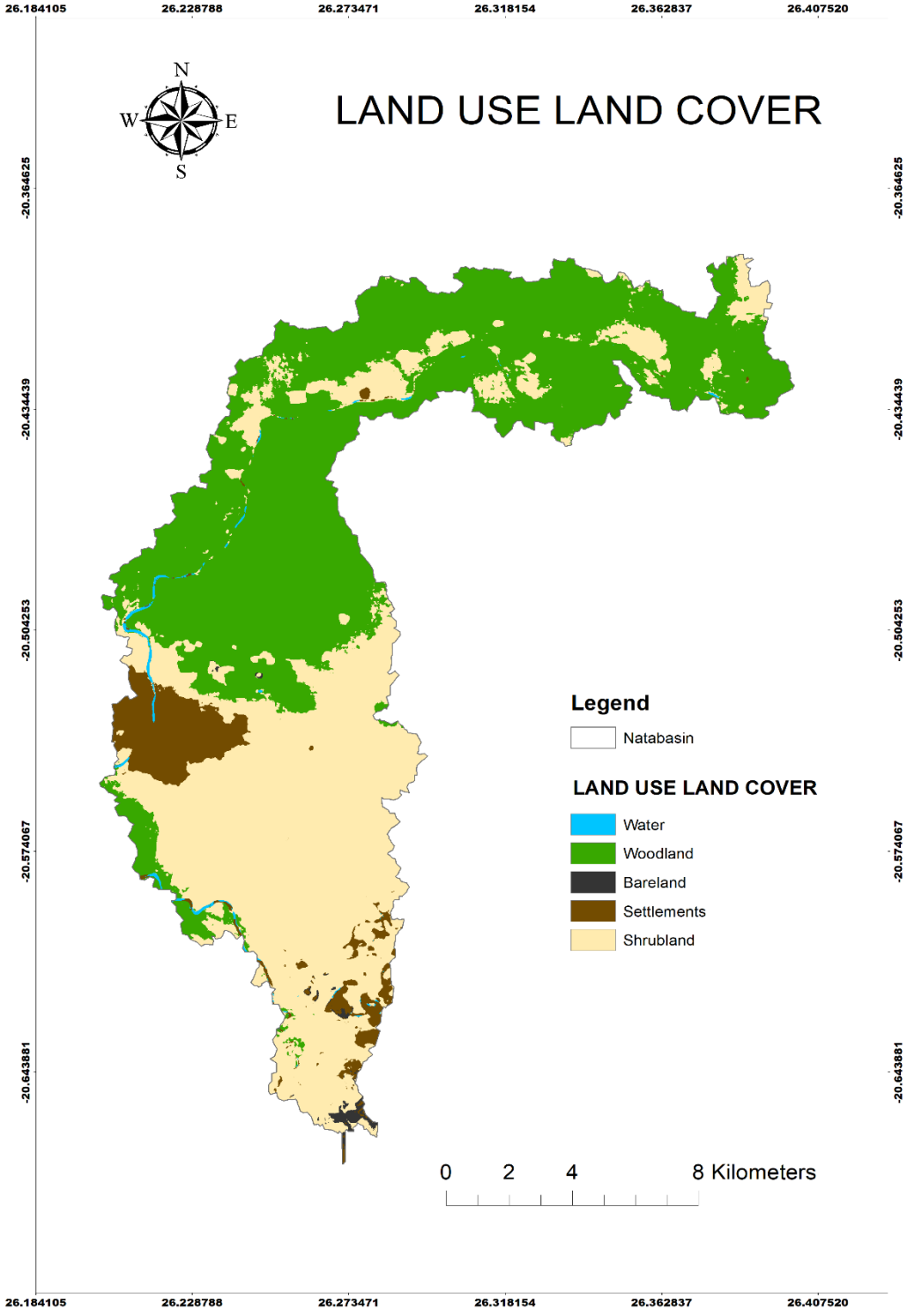


Figure 19: Land cover/land use for the study area

4.2.3.1 Reclassified land cover/land use

Impermeable surfaces, such as roads and buildings, are identified on the land use map as being more susceptible to floods. A lower risk rating was assigned to agricultural land that is covered in natural vegetation. Based on the probable effects of each land use type on flood risk, the land use map can be classed, with natural vegetation cover being rated as having a reduced risk and impermeable surfaces being rated as having a very high risk.

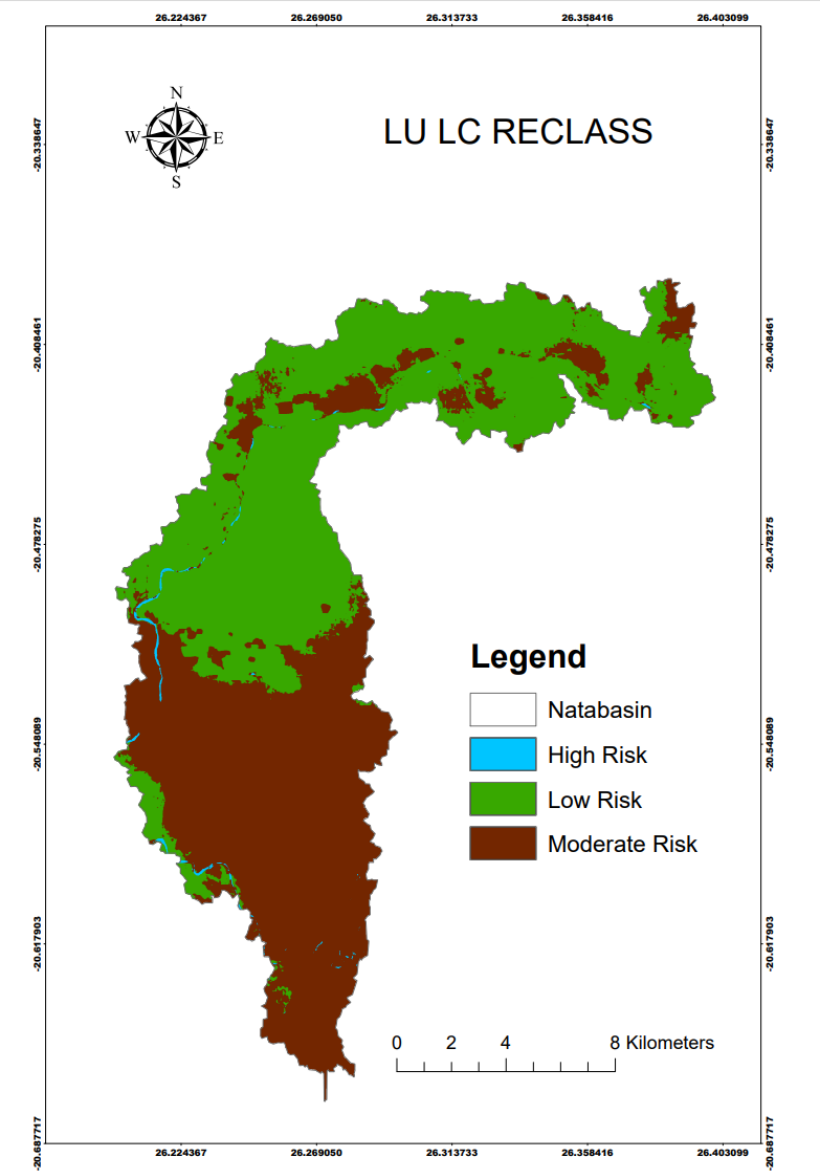


Figure 20: Reclassified Land cover/land use for the study area

4.2.4 Soil type

The rescue crews require the most recent data on the impacted soil type to know which structures are most likely to experience damage. Also, to understand which soils might become polluted, degrade, or lose their fertility after a flood. Figure 21 below shows the soil distribution in our river basin.

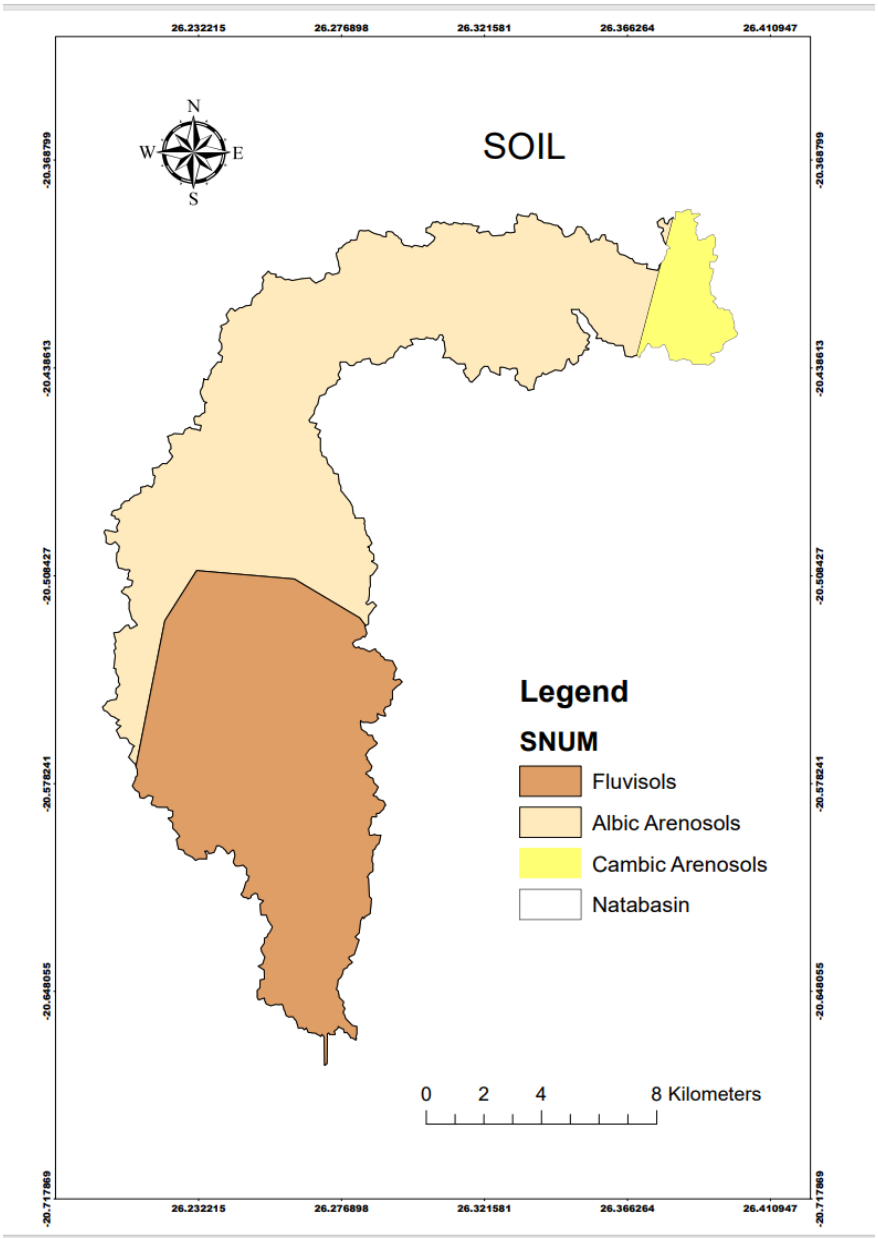


Figure 21: Soils in the study area

4.2.4.1 Reclassified soils

Due to their low infiltration rate, two of the higher soils, or arenosols, which make up 58% of the basin, are classified as having a high to moderate flood hazard due to their low permeability. Due to their high infiltration rate, locations with sandy soil may be identified on the soil type map as having a decreased risk of floods. The risk of flash floods, however, may be higher in places with extremely erodible soil. Sandier soils are assessed as having a lesser danger of flooding than highly erodible soils, and the soil type map can be classed based on the degree of sandiness and erosion potential. The following type of soil is called a fluvisol, and it makes up 41.9% of the basin. This soil is classified as having a very high flood hazard because of its high clay concentration, which results in a low infiltration rate. The region covered by these soils is shown in brown on the soil reclass map in the southern portion of the research area, which is the region near the pan.

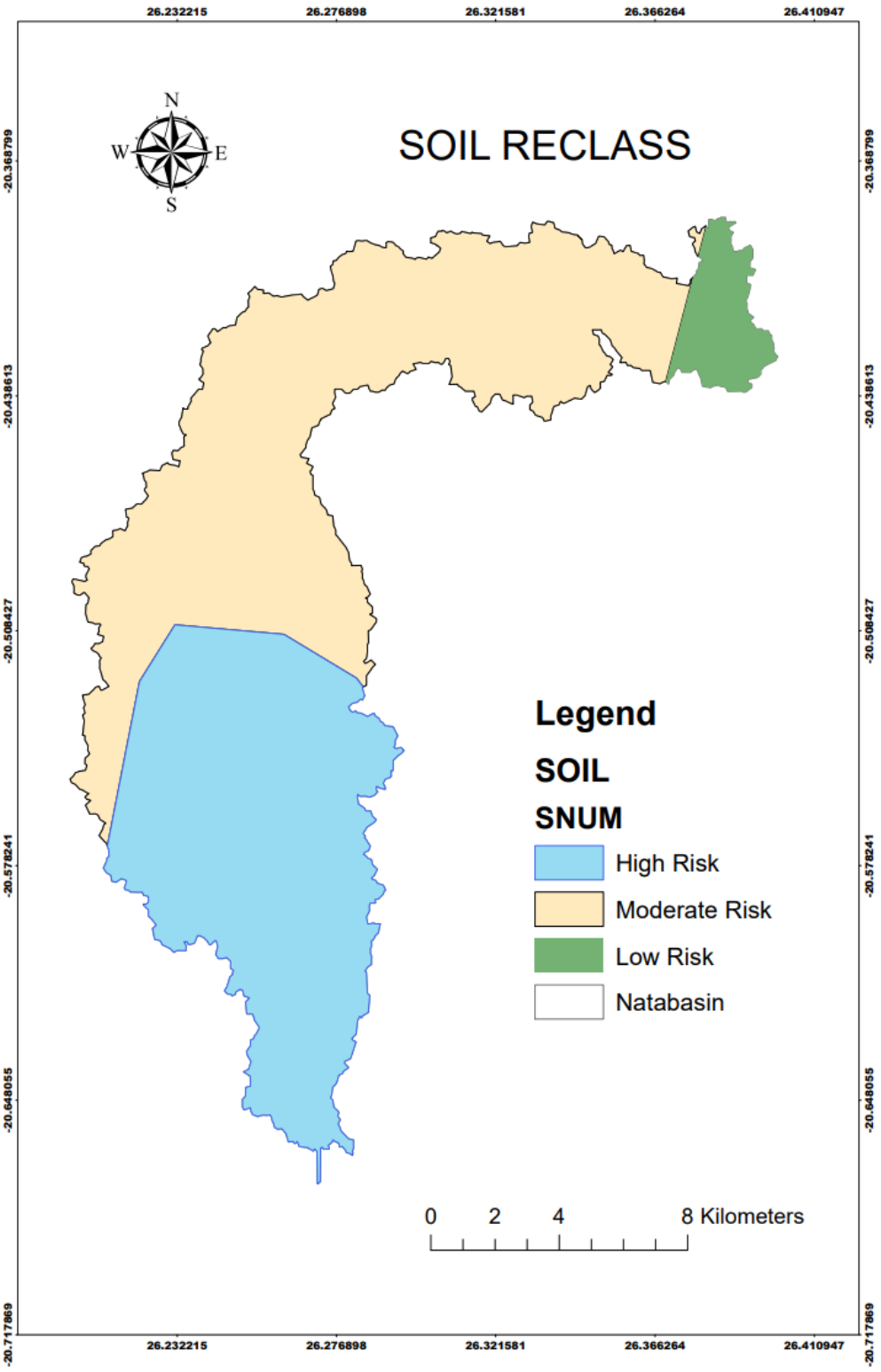


Figure 22: Reclassified Soils in the study area

4.3 Spatial modelling of flood risk

The weighted interaction rate of the flood risk maps displayed in Figure 23 is used to construct the possible flood risk map. Using Reclassification, flood risk and vulnerability in the eastern part of Makgadikgadi pans was modelled for all parameter discussed in sections above. Studies also showed that increased infrastructure, commercial, and residential construction has increased the number of impermeable surfaces, which has increased storm water runoff. Also, it was noted that inadequate culvert and stream channel capacities and blockade of flows by structures built through ordinary river flow all contribute to floods.

The % coverage of hazard zones is shown in Table 9. The generated map indicates that all regions within the research area experience some level of flooding. As seen in the table, stream buffer has the highest weight with 35%, followed by Land use and Elevation at 30 and 24 percent, respectively. Flow direction, slope and soil type have weights of 3, 3 and 5 respectively. The literature review, expert opinions, and assessments of the local context were used to determine the values and weights for each parameter.

As an example the 30% weight assigned to the land use parameter in the flood risk assessment was determined through a combination of three factors. First, the literature review highlighted the significant influence of land use on flood risk, especially in urbanised and impermeable areas, where the lack of natural drainage exacerbates flooding. Second, expert opinions from professionals in hydrology and land use planning contributed valuable insights on how different land use types, such as urbanisation and agriculture, affect the likelihood and severity of floods. Finally, an assessment of the local context involved analysing local land use data, including satellite imagery and maps, to better understand the specific distribution of land

use types in the study area and their direct impact on flooding. These combined factors led to the assignment of the 30% weight, recognizing land use as a critical parameter in flood risk modeling.

Table 9 Weighted Overlay Criteria for Study Parameters

Parameter	Land Associated to Risk (km2)	Rating Index	Weights (%)
Elevation	67.28	High Risk	24
	74.56	Moderate Risk	
	63.18	Low Risk	
Flow Direction	7.75	High Risk	3
	66.85	Moderate Risk	
	112.94	Low Risk	
Slope	67.35	High Risk	3
	74.54	Moderate Risk	
	63.10	Low Risk	
Stream Buffer (distance from the river)	136.89	High Risk	35
	59.31	Moderate Risk	
	8.70	Low Risk	
Land use	1.86	High Risk	30

	84.89	Moderate Risk	
	118.27	Low Risk	
Soil type/structure	86.51	High Risk	5
	108.69	Moderate Risk	
	9.69	Low Risk	

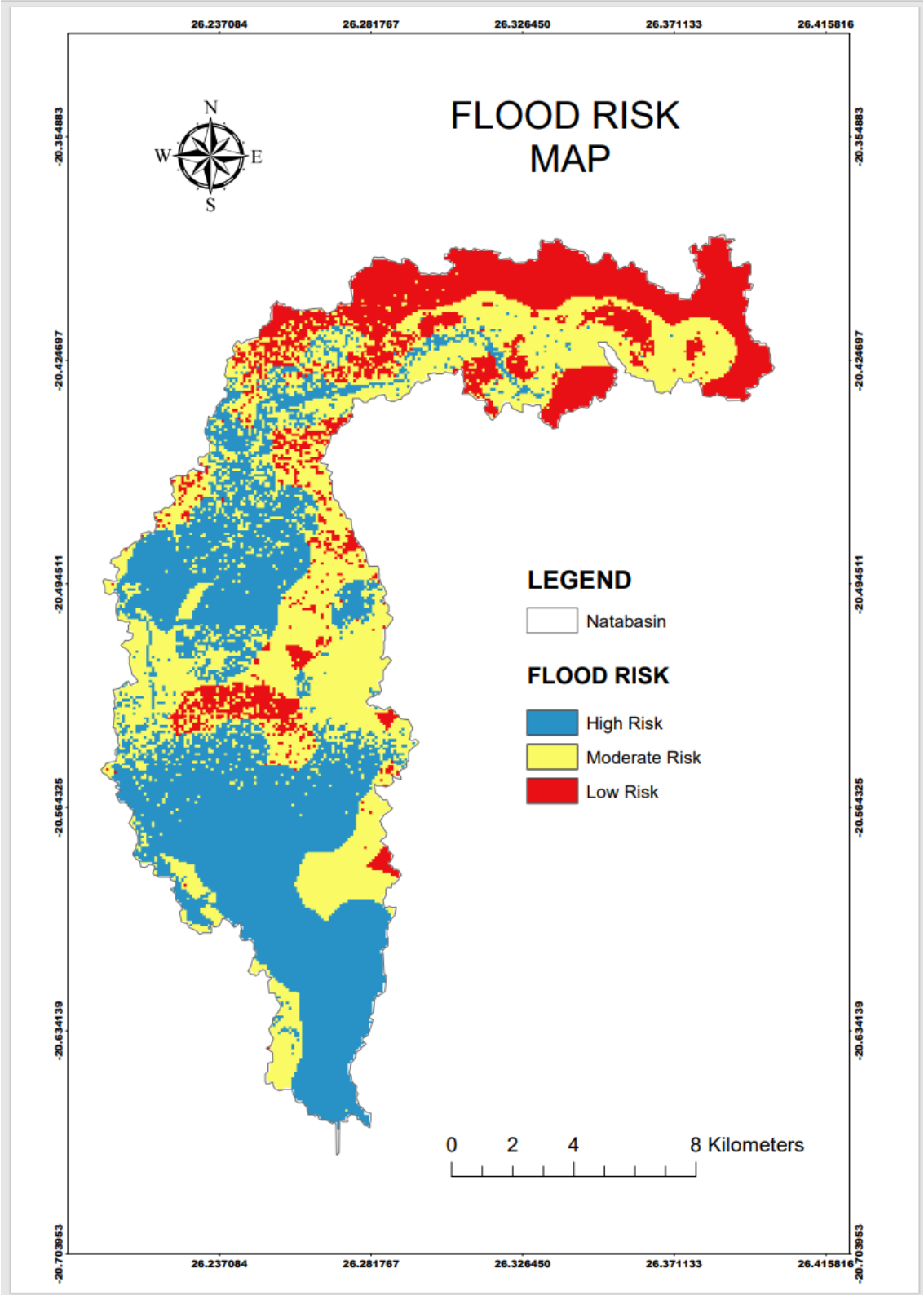


Figure 23: Flood risk Map

Table 9 above was used to create the results in Figure 23, which display various risk patterns for the research area. Table 10 displays the data. According to the table below, approximately 41.3% of the study area has high risk flooding; these areas are located on the study area's low-lying sections and have loam sandy soils. Four percent of the low flood risk locations are in the northern portion of the study. The Nata settlement is situated in the center of the research region, which includes 54.7% of the areas under moderate risk of flooding. As a result, these locations are vulnerable to flooding during periods of intense precipitation.

Table 9 was used to create Figure 23 by first preparing and reclassifying raster data for flood-related parameters, such as land use, elevation, flow direction, slope, and soil type. Each of these parameters was assigned a weight based on its importance in contributing to flood risk, as outlined in the table. The weighted overlay tool in ArcGIS was then applied to combine the reclassified layers, with each pixel in the layers multiplied by its corresponding weight. The results were summed to calculate the overall flood risk across the study area, which was then classified into high, moderate, and low flood risk zones. The final flood risk map in Figure 23 was generated, visually representing these categories across the research region, with high-risk areas in red, moderate-risk in yellow, and low-risk in green. This process demonstrated the integration of the weighted parameters to provide a comprehensive flood risk assessment for the study area.

Table 10: Flood risk map statistics

RISK LEVEL	AREA (km2)	Percentage
High Risk	83.24	41.3%
Moderate Risk	110.11	54.7%
Low Risk	7.98	4%

4.4 Sensitivity analysis

Satellite photos of the study area were examined to determine whether the map produced by the MCA procedure accurately depicts the flood-prone areas there but before that the sensitivity of the MCA was analysed by using the scenarios below.

As a process of validation, the sensitivity analysis was carried out on extra two distinct scenarios, each of which is modeled separately with a particular modification in one or two factors, as indicated in Table 11 and Figure 24. By altering a parameter's input and observing the result, the goal was to determine whether the model accurately captures reality. Figure 24's sensitivity analysis for flood risk reveals that, in comparison to the initial flood risk values, there is little variation in the high-risk locations for either scenario.

Table 11 : Sensitivity analysis scenarios

Criterion	First	Second
Elevation	30	35
Flow Direction	3	3
Slope	3	3
Stream order (Buffer from river)	24	30
Land Use	35	24
Soil type	5	5
Total	100	100

Table 11 and figure 24 elaborate further the changes happening to the MCA map when the weights are changed. Scenario 1 and Scenario 2 represent alternative flooding scenarios that were created by altering the weights of the criteria used in the flood risk analysis. In Scenario 1, the weights for specific parameters such as elevation and stream order (buffer from river) were adjusted to simulate different flood risk outcomes. Scenario 2, on the other hand, involved a further adjustment of these weights to explore the effect of different parameter combinations on the flood risk map. The justification for these two scenarios is to assess how variations in the criteria weights could influence flood risk categorisation and the spatial distribution of flood-prone areas.

The information is provided for the entire area as well as for the three flood risk categories of High Risk, Moderate Risk, and Low Risk. All three scenarios share a common total area of 201 km². There is a minor rise under Scenario 1 compared to the baseline scenario, but a slight decrease under Scenario 2. This is true for the High-Risk category. There is a reduction in the area covered by Scenario 1 for the Moderate Risk category, but an increase under Scenario 2. The area covered by both Scenario 1 and Scenario 2 has somewhat respectively increased and decreased for the Low-Risk category. Overall, each scenario's area changes very little, with Scenario 2's Moderate Risk category decrease by 2.1 km² as the largest change as seen on table 12 and figures 24.

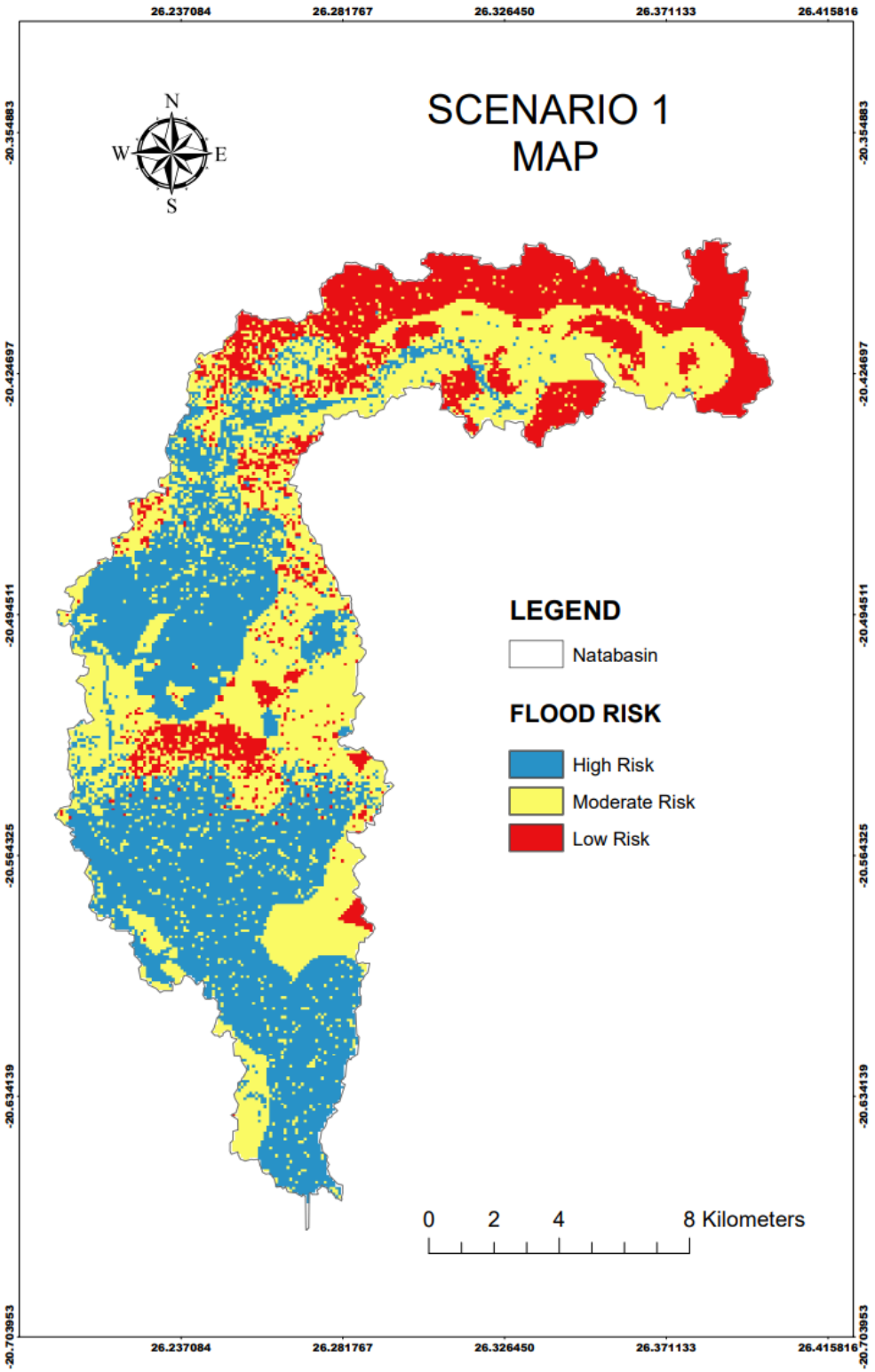


Figure 24.a: Flood risk Maps for scenarios 1

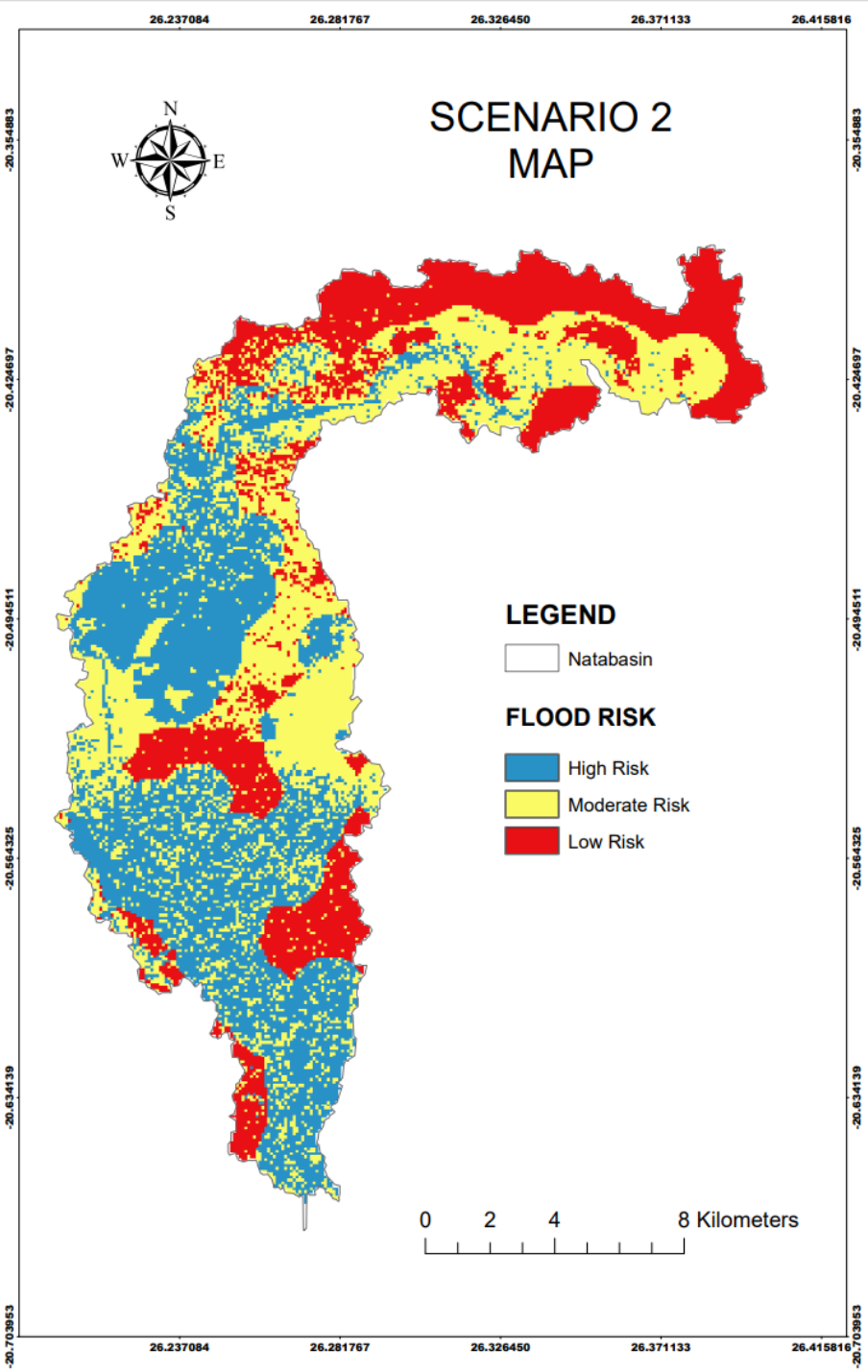


Figure 24.b: Flood risk Maps for scenarios 2

Table 12: Scenarios for sensitivity analysis statistics comparison

Flood risk level	Flood risk map area(km2)	Scenario 1 area (km2)	Scenario 2 area (km2)
High Risk	83.24	83	83
Moderate Risk	110.11	108	110
Low Risk	7.98	10	8
Total	201	201	201

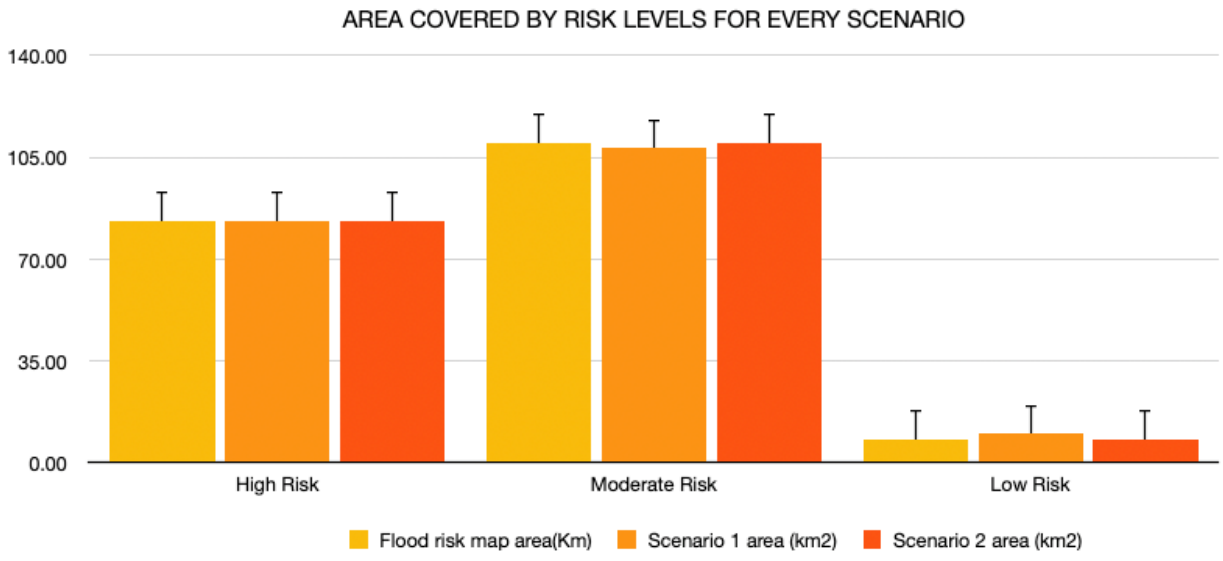


Figure 25: Flood risk levels for scenarios compared in bar chart

4.5 Flooding extent mapping

The following images are the outcome of binarising and performing geometric rectification on satellite images.

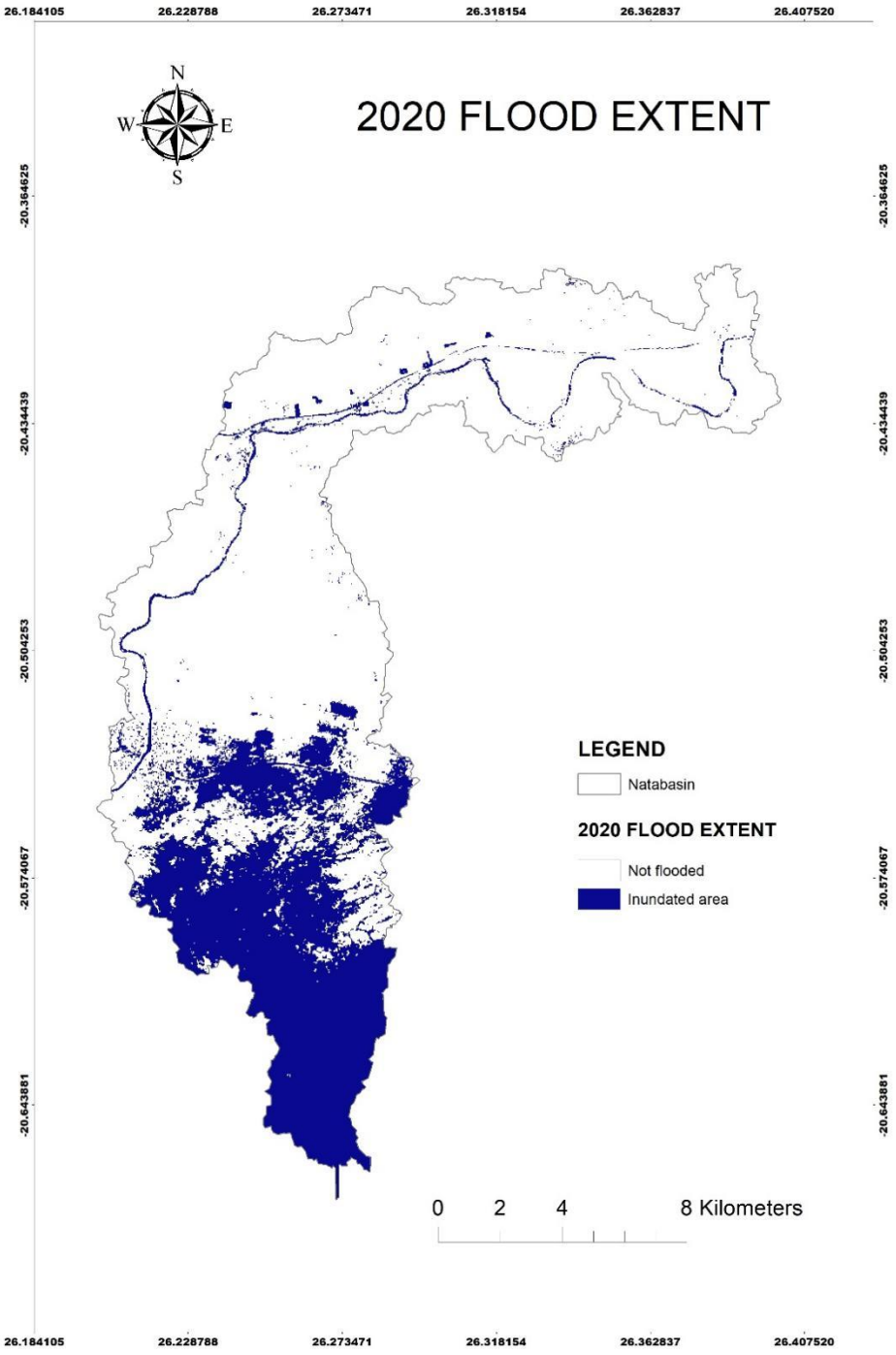


Figure 26: Water extractions from Landsat images during flooding in 2020

The white color on the map (figure 26) reflects other types of land cover, whereas blue on the map represents water. The map was created using a satellite image that was taken in February 2020, a few days following flooding. It's noticeable that there is a fair amount of water on this map, which provides a better if still imperfect portrayal of places that have flooded.

The flood danger map produced by the MCA process is superimposed on the flood extent map in Figure 27 below. It was predicted that the blue color, which represents the extracted water from the Landsat images, would match the red and yellow colors, which represent the high and moderate levels of flood from the MCA. These two are observed to be matched by the water, albeit more to the mild degree of inundation. Among the many possible reasons for this are the different soil types' of moisture and clay contents as well as the absence of current satellite images of the flooding event. These issues should be investigated in future research.

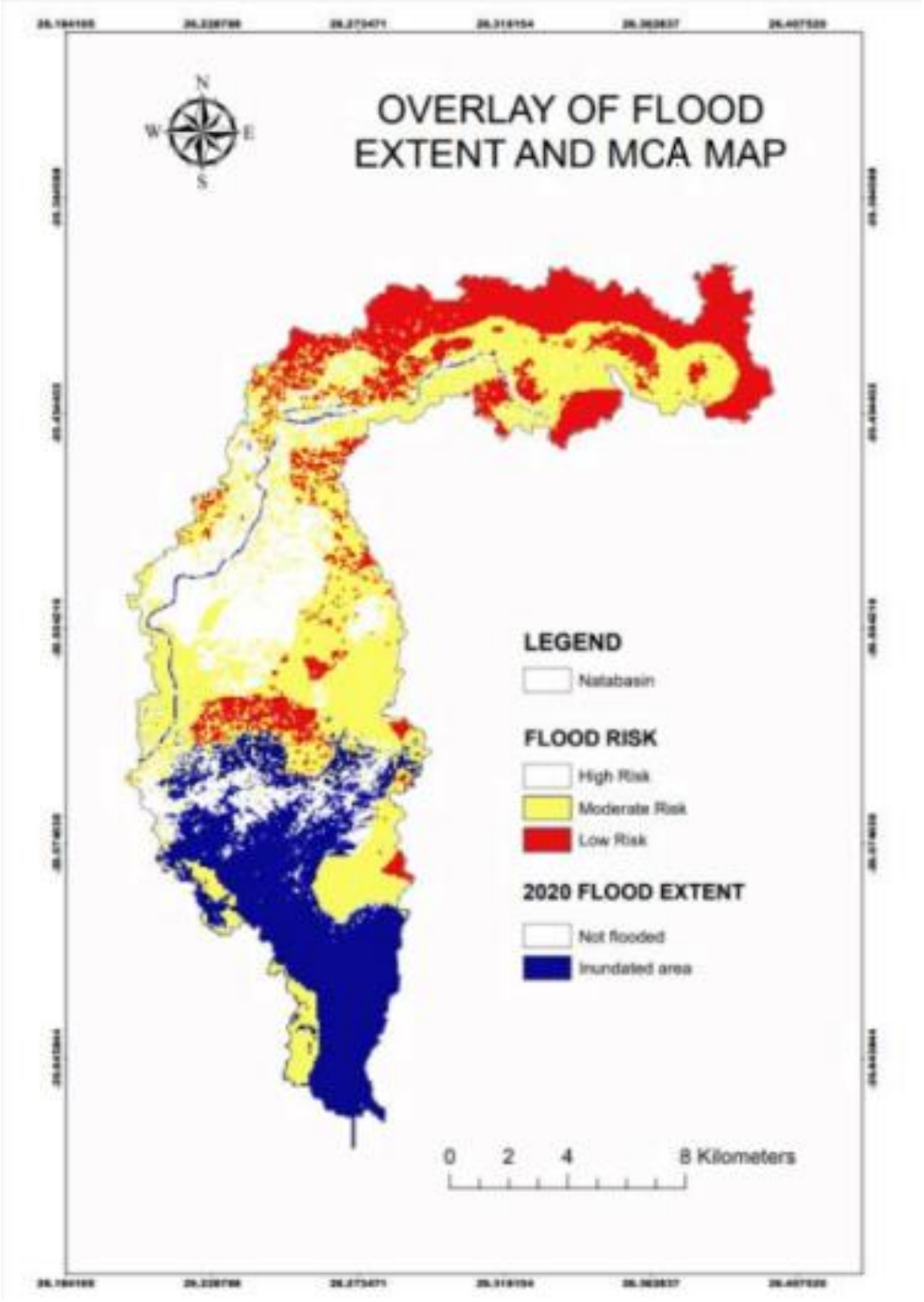


Figure 27: Overlay of the flood risk map and flood extent map.

Chapter 5

DISCUSSION AND CONCLUSION

5.1 Discussions

5.1.1 Flood Frequency through Gumbel Distribution

The first objective of this thesis was to determine the size and frequency of floods in Botswana, using Nata as a case study. This analysis was aimed at understanding not only the occurrence of floods but also their recurrence intervals. To achieve this, return periods were computed based on total yearly rainfall data collected from meteorological stations in the research area. The findings revealed that there is a 100% likelihood of an annual precipitation of 300.59 mm occurring once every 32 years, while an annual precipitation of 63.28 mm is expected to occur annually. These results offer vital insights for flood risk management and planning in Botswana, particularly in regions like Nata that are prone to flood events.

The application of the Gumbel distribution method, validated using historical flood data, produced reliable results. However, certain limitations inherent in the method need to be acknowledged. The Gumbel distribution assumes that the data fits a specific statistical distribution, which may not always align with real-world scenarios. Furthermore, the method may not adequately estimate extreme flood events that fall outside the range of historical data. Discussing these limitations is essential to provide a balanced perspective, highlighting both the strengths and constraints of this approach in flood frequency analysis.

The Results and Analysis chapter emphasised the application of Gumbel distribution in predicting flood occurrences based on historical rainfall data. By achieving this objective, the study offers critical insights into flood dynamics in Botswana, serving as a foundation for developing disaster preparedness strategies and enhancing resilience to flooding. The analysis for Objective 1 establishes a systematic approach to understanding flood frequency, underlining the importance of integrating historical rainfall data with predictive models for comprehensive flood risk management.

5.1.2 Flood Risk Assessment Tool Using Geospatial Techniques

Through the integration of multiple GIS-based tools, a flood risk map was developed to identify areas susceptible to flooding within the study area. This map serves as a product of the flood risk assessment process, combining various geospatial datasets, such as elevation, slope, land use, and soil type, to evaluate flood hazards in Nata. The purpose of this tool is to illustrate how geospatial data and analyses can be utilized to predict and assess flood risks. In this context, the focus is on the interaction between environmental parameters and their spatial distribution, which ultimately influences flood patterns in the study area.

The results presented in Section 4.3 highlight the effectiveness of geospatial techniques in delineating flood-prone areas. For instance, the analysis revealed that areas with low elevation and loam sandy soils were highly susceptible to flooding, particularly during periods of intense precipitation. The weighted overlay method allowed for the integration of multiple datasets, enabling the identification of high-risk, moderate-risk, and low-risk zones.

5.1.2.1 Elevation and Slope

The Nata River basin is a low-lying region with a predictable slope, as can be seen in chapter 4. The lowest point in the basin is in the south when it meets the Makgadikgadi pans. Then, this area is regarded as having the highest risk of any in the basin. A total area of approximately 63 km² for both slope and elevation is covered by low-risk areas, 67km² for high risk and 74.5 km² for moderate risk areas. Alawadi et al. (2023) state that while the water level does not rise to dangerously high levels in cities with flat topography, the flow is rather sluggish, and you can see people driving through it. Conversely, flat surfaces have a very slow runoff and retain water from upstream or elevated ground. Furthermore, flat areas have a high risk of flooding, according to Alawadi et al. (2023), because rivers that cause flooding are formed when water flows from mountainous hillside into lower terrain. Therefore, when making plans for developments in this area, the topography of the Nata basin should be considered.

5.1.2.2 Hydrological indicators

Flood danger is significantly influenced by stream order, which is the placement of a specific stream or river within a wider network of waterways (Antzoulatos, 2022). The distance between the river and the surrounding land, known as the buffer distance from the river, is crucial in evaluating the level of risk. According to this study, areas within a high-risk buffer are up to 136.89 Km²; moderate risk areas are 59.31 Km²; and low risk zones are 8.70Km².

5.1.2.3 Land Use

Residential and business areas close to water features including tiny dams, ponds, and streams along the Nata River are put under an emergency because of this. Such information can

be very helpful in determining which rivers might have an impact on the dam. Risk estimates can also be made for the nearby people and property (UNISDR, 2015; Tasri, 2021). It can be utilised in a GIS environment for early warning systems and flood predictions in the future. In this study the land cover area with high and moderate risk probability covers up to 86.75 Km². The remaining 118.27 Km² land cover is deduced to have low risk probability of being flooded.

5.1.2.4 Soil

When a flood occurs, erosional activity peaks, soil nutrients are lost in significant quantities, pesticides from agricultural fields are released, and industrial waste is dumped into lakes together with the floodwater (Keagakae, 2020). Soil type/structure is also a significant variable that influences flood risk (Klemas, 2015). This study shows that soil types with high risk fall within an area covering 86.51 Km², while those soil types/structures with moderate risk cover 108.69 Km², and those with low risk 9.69 Km². The presence of loam sandy soils in high-risk zones indicates poor drainage capacity, which exacerbates flooding during heavy rainfall. Addressing this issue requires the implementation of soil management strategies, such as improving drainage systems or adopting land-use practices that minimize runoff.

5.2 Weighted overlay analysis

In flood-prone locations, flood risk mapping is an important part of appropriate land use planning because it produces easily readable and accessible maps that allow planners and overseers to identify high-risk areas and prioritise response actions (Chan, 2022). This is why the study's goal was to map Nata River basin’s cumulative flood risk. The utilisation of geospatial expertise is crucial in flood assessment, particularly as the adoption of technology increases globally. As a

result, this method can help decision makers assess and evaluate flooding occurrences in urban areas without having to wait for the hazard to materialise (Ouma and Tateishi, 2014). The multi-criteria analysis approach utilised in mapping flood hazard zones needed the combination of the following recognized decision criteria, elevation, land cover, slope, flow direction, stream buffer, and soil geology. Several GIS operations and image processing techniques were included in the methodology. And the resulting map suggests that approximately 41.3 percent of the research region is likely to encounter a high degree of flood, 54.7 percent has a moderate likelihood of getting inundated and only 4 percent has a low-risk probability. While the approach effectively combines multiple datasets to generate a flood risk map, its reliance on predefined weights introduces subjectivity. Future studies could explore alternative weighting methods, such as machine learning algorithms, to enhance accuracy.

5.3 Conclusion

This study examined flood frequency using the Gumbel distribution method and employed geospatial techniques to create flood risk maps for the Nata River Basin. By integrating long-term rainfall records with geospatial datasets, the research provided a practical and efficient strategy for mapping flood risk and vulnerability in the region. The analysis of rainfall patterns, including the frequency, intensity, and recurrence intervals, enabled the assessment of flood risk and highlighted the importance of historical flood data in understanding flooding dynamics. Specifically, the study demonstrated that high total precipitation events, though rare, are associated with severe flooding, posing significant risks to communities and infrastructure.

Objective 1, focused on flood frequency analysis, was achieved by analyzing annual rainfall records and applying the Gumbel distribution. The results indicated a 100% likelihood of

annual precipitation of 300.59 mm occurring every 32 years, alongside a higher probability of smaller annual precipitation events. These insights contribute to Botswana's limited data on flood recurrence intervals and enhance preparedness strategies by providing a predictive framework for flood management.

Objective 2, which involved assessing flood hazards using geospatial techniques, was met through the development of flood risk maps. Using a combination of digital elevation models, land use data, soil characteristics, and hydrological indicators such as flow accumulation and stream buffers, the study identified high-risk, moderate-risk, and low-risk zones. These maps offer valuable tools for floodplain management, urban planning, and emergency response, providing stakeholders with the ability to visualize and assess flood impacts effectively.

The findings have several implications for flood risk management in Botswana. The integration of geospatial techniques enables planners and decision-makers to identify flood-prone areas, establish emergency response plans, and develop guidelines for infrastructure and settlement planning in vulnerable zones. For instance, overlaying flood maps with infrastructure data can pinpoint areas of immediate risk, facilitating targeted mitigation measures and resource allocation during emergencies.

In conclusion, this research successfully achieved its objectives, contributing to the understanding of flood risks in the Nata River Basin. The integration of flood frequency analysis with geospatial tools highlights the importance of data-driven approaches in addressing flood hazards. These findings not only add to the body of knowledge on flood risk management in

Botswana but also provide actionable insights for policymakers and stakeholders to enhance disaster preparedness and resilience.

5.4 Further study areas

Further study directions may be suggested by the validation of the Gumbel distribution approach using historical flood data. For estimating flood magnitudes and frequencies, it might be helpful to compare the Gumbel distribution method's performance with other approaches. In order to judge the method's generalisability, it may also be helpful to investigate how it performs in various places with various climatic circumstances.

It is vital to map different danger zones for town planning and floodplain management in order to establish emergency response methods and specify development guidelines. Maps representing flood extents are clearly beneficial for displaying the area impacted by a certain historical flood or a flood with a specific likelihood of recurring (Bentivoglio, 2022). Maps for each flood level can be simply made using GIS once the anticipated flood levels have been identified. In a planning scenario, GIS tools may readily perform various land use-based overlay assessments. Moreover, maps of the final analysis can be produced. It is possible to determine whether infrastructure is immediately at risk when overlayed on an infrastructure database. For effective hazard management, a visual representation of the numerical impact analysis results can be beneficial (Tasri, 2021).

Further research is required to create global exclusion layers for arid regions. For end users with limited time for action, the integration of this exclusion layer with the Sentinel-1 Flood Service would result in improved classification accuracy with little computing time.

References

African Centre of Meteorological Applications for Development (ACMAD): Weekly monitoring and forecasts of heavy rains 18-25 February 2013; Hydrological Services Namibia: Daily Flood Bulletin 17 Feb 2013. https://acmad.org/index.php/weather-watch-and/

African Region Disaster Management Team. (2010). "Report on the status of disaster risk reduction in sub-Saharan Africa", The International Bank for Reconstruction and Development/The World Bank Washington, D.C. https://daraint.org/wp-content/uploads/2012/01/2010_Status_DRR_Africa.pdf

Afzal, M.A.; Ali, S.; Nazeer, A.; Khan, M.I.; Waqas, M.M.; Aslam, R.A.; Cheema, M.J.M.; Nadeem, M.; Saddique, N.; Muzammil, M.; et al. (2022). "Flood Inundation Modeling by Integrating HEC–RAS and Satellite Imagery: A Case Study of the Indus River Basin". Water, 14, 2984. https://doi.org/10.3390/w14192984

Akinyemi, F. O. (2021). "Vegetation trends, drought severity and land use-land cover change during the growing season in semi-arid contexts". Remote Sensing, 13(5), 1–20. https://doi.org/10.3390/rs13050836

Alawadi, W.A., Raheem, Z.A.H.A. & Yaseen, D.A. (2023). Use of remote sensing techniques to assess water storage variations and flood-related inflows for the Hawizeh wetland. Environ Monit Assess 195, 1246. https://doi.org/10.1007/s10661-023-11838-x

Andráško, I; Klemešová, K. D; Dvořák, P. (2024)"Clarifying “flood experience”: A novel conceptual model demonstrates how a flood experience emerges and what determines its intensity and character". International Journal of Disaster Risk Reduction. https://doi.org/10.1016/j.ijdrr.2023.104150.

Antzoulatos, G., Kouloglou, I. O., Bakratsas, M., Moumtzidou, A., Gialampoukidis, I., Karakostas, A., Lombardo, F., Fiorin, R., Norbiato, D., Ferri, M., Symeonidis, A., Vrochidis, S., & Kompatsiaris, I. (2022). Flood Hazard and Risk Mapping by Applying an Explainable Machine Learning Framework Using Satellite Imagery and GIS Data. Sustainability (Switzerland), 14(6). https://doi.org/10.3390/su14063251

Anusha, N; Bharathi, B. (2020). "Flood detection and flood mapping using multi-temporal synthetic aperture radar and optical data",The Egyptian Journal of Remote Sensing and Space Science, 23(2),207-219, https://doi.org/10.1016/j.ejrs.2019.01.001

Aroca-Jiménez E, Bodoque JM, García JA. (2020) “How to construct and validate an Integrated Socio-Economic Vulnerability Index: Implementation at regional scale in urban areas prone to flash flooding”. Sci Total Environ. 746:140905. http://doi:10.1016/j.scitotenv.2020.140905

Atanga, R; Tankpa, V. (2022). “Geospatial analysis of flood emergency evacuation sites in Accra”. Jàmbá: Journal of Disaster Risk Studies, 14(1). https://doi.org/10.4102/jamba.v14i1.1172

Atanga R. A; Tankpa V; Acquah I. (2023). “Urbanization and flood risk analysis using geospatial techniques”. PLoS ONE 18(10): e0292290. https://doi.org/10.1371/journal.pone.0292290

Bertola, M., Viglione, A., Lun, D., Hall, J., & Blöschl, G. (2020). Flood trends in Europe: Are changes in small and big floods different? Hydrology and Earth System Sciences, 24(4), 1805–1822. https://doi.org/10.5194/hess-24-1805-2020

Bentivoglio, R., Isufi, E., Jonkman, S. N., Taormina, R. (2022). "Deep learning methods for flood mapping: a review of existing applications and future research directions". In Hydrology and Earth System Sciences (Vol. 26, Issue 16, pp. 4345–4378). Copernicus GmbH. https://doi.org/10.5194/hess-26-4345-2022

Chan, S. W; Abid, S. K; Sulaiman, N; Nazir, U; Azam, K.(2022). "A systematic review of the flood vulnerability using geographic information system". Heliyon. 8(3):e09075. http://doi:10.1016/j.heliyon.2022.e09075.

De Groeve, T. (2010). Flood monitoring and mapping using passive microwave remote sensing in Namibia. Geomatics, Natural Hazards and Risk, 1(1), 19–35. http://https://doi.org/10.1080/19475701003648085

Dewan, A.M; Kankam-Yeboah, K; Nishigaky, M. (2014). Using synthetic aperture radar (SAR) data for mapping river water flooding in an urban landscape: a case study of greater Dhaka, Bangladesh J. Jpn. Soc. Hydrol. Water Resour., 19 (1), pp. 44-55. http://DOI:10.3178/jjshwr.19.44

Eldho, T. I.; Zope, P. E.; Kulkarni, A. T. (2018). "Chapter 12 - Urban Flood Management in Coastal Regions Using Numerical Simulation and Geographic Information System, Editor(s):

Pijush Samui, Dookie Kim, Chandan Ghosh," Integrating Disaster Science and Management, 205-219, https://doi.org/10.1016/B978-0-12-812056-9.00012-9.

Elias, E., Seifu, W., Tesfaye B., and Girmay, W. (2018). Land Use Land Cover Changes and their impact on the lake ecosystem of the Central Rift Valley of Ethiopia. Cogent Food & Agriculture 5, no. 1. http://doi:10.1080/23311932.2019.1595876.

European Commission. (2007). "Directive 2007/60/EC of the European Parliament and of the Council of 23 October, 2007 on the assessment and management of flood risks." Official Journal of the European Union, vol. L288, p. 27. http://data.europa.eu/eli/dir/2007/60/oj

FAO (2016). Map Accuracy Assessment and Area Estimation: A Practical Guide. Food and Agriculture Organization of the United Nations, Rome. https://openknowledge.fao.org/handle/20.500.14283/I5601E

Gan, T.Y; Zunic, F; Kuo, C.C; Strobl, T. (2012). Flood mapping of Danube river at Romania using single and multi-date ERS2SAR images Int. J. Appl. Earth Obs. Geoinf., 18, pp. 69-81 http://DOI:10.1016/j.jag.2012.01.012

Ganjirad, M., & Delavar, M. R. (2023). "Flood risk mapping using random forest and support vector machine". ISPRS Annals of the Photogrammetry, Remote Sensing and Spatial Information Sciences, 10(4/W1-2022), 201–208. https://doi.org/10.5194/isprs-annals-X-4-W1-2022-201-2023

Gogoi, P., Patnaik, S.K. (2022). "Remote Sensing and GIS Application in Flood Management: A Case Study of the Jiadhal River Basin of Dhemaji District, Assam, India". In: Bhunia, G.S., Chatterjee, U., Lalmalsawmzauva, K., Shit, P.K. (eds) Anthropogeomorphology. Geography of the Physical Environment. Springer, Cham. https://doi.org/10.1007/978-3-030-77572-8_5

Hernández-Hamón, H., Ramírez, P. Z., Zaraza, M., & Micallef, A. (2023). "Google Earth Engine app using Sentinel 1 SAR and deep learning for ocean seep methane detection and monitoring". Remote Sensing Applications: Society and Environment, 32, 101036. https://doi.org/10.1016/j.rsase.2023.101036

Honda K. C., Francis X. J., and Sah V. P. (1997). Flood monitoring in central plain of Thailand using JERS-1 SAR data. Proc. 18th Asian Conference of Remote Sensing, Malaysia. https://a-a-r-s.org/proceeding/ACRS1997/Papers/DIS97-2.htm

IFRC, (2013). Botswana: Floods - Jan 2013 [Online]. Available: Https://Reliefweb.Int/Disaster/Fl-2013-000013-Bwa.

IFRC, (2017). Emergency Plan of Action Final Report Botswana: Cyclone Dineo. Available: https://adore.ifrc.org/Download.aspx?FileId=179525.

Jonah, I. (2024). "Flood Mapping of Federal Polytechnic Ekowe, Bayelsa State, Using Remote Sensing and GIS Tools". https://doi.org/https://www.researchgate.net/publication/380752411

Keagakae, K. (2020). Geospatial assessment of land degradation: a case study of Selebi phikwe and Mmadinare area, Botswana. University of Botswana, Botswana. Msc thesis published.

Klemas, V. (2015). "Remote Sensing of Floods and Flood-Prone Areas: An Overview," Journal of Coastal Research, 31(4), 1005-1013, https://doi.org/10.2112/JCOASTRES-D-14-00160.1

Krichen, M; Abdalzaher, M. S; Elwekeil, M; Fouda, M. M. (2023) "Managing natural disasters: An analysis of technological advancements, opportunities, and challenges", Internet of Things and Cyber-Physical Systems, 99-109, https://doi.org/10.1016/j.iotcps.2023.09.002.

Lambin, E.F., Geist, H.J., & Lepers, E. (2003). Dynamics of land-use and land-cover change in tropical regions. Annual review of environment and resources, 28, 205-241. https://doi.org/10.1146/annurev.energy.28.050302.105459

Leon, J. X., Phinn, S. R., Hamylton, S., & Saunders, M. I. (2013). Filling the 'white ribbon' – a multisource seamless digital elevation model for Lizard Island, northern Great Barrier Reef. International Journal of Remote Sensing, 34(18), 6337–6354. https://doi.org/10.1080/01431161.2013.800659

Lillesand, T. M, Kiefer, R.W., and Chipman, J. W. (2014). Remote Sensing And Image Interpretation. John Wiley & Sons. http://ISBN:978-1-118-34328-9

Long, S; Fatoyinbo, T. E. and Policelli, F. (2014). Flood extent mapping for Namibia using change detection and thresholding with SAR, Environmental Research Letters, vol. 9, no. 3, p. 035002. http://DOI10.1088/1748-9326/9/3/035002

Mashao, F.M.; Mothapo, M.C.; Munyai, R.B.; Letsoalo, J.M.; Mbokodo, I.L.; Muofhe, T.P.; Matsane, W.; Chikoore, H. (2023). "Extreme Rainfall and Flood Risk Prediction over the East Coast of South Africa". Water, 15(1), 50. https://doi.org/10.3390/w15010050

McCormack, T., Campanyà, J., Naughton, O. (2022). A methodology for mapping annual flood extent using multi-temporal Sentinel-1 imagery. Remote Sensing of Environment, 282. https://doi.org/10.1016/j.rse.2022.113273

McGrath, H. (2017) . "Web-based flood risk assessment-Rapid, user-friendly tools leveraging open data," MSc Thesis, University of Brunswick, Canada. https://gge.ext.unb.ca/Pubs/TR308.pdf

Natarajan, S., Radhakrishnan, N. (2021). Flood Risk Assessment for a Medium Size City Using Geospatial Techniques with Integrated Flood Models. 39-77. http://10.1007/978-3-030-67865-4_3

Ogashawara, I; Curtarelliand, M.P; Ferreira, C.M. (2013). The use of optical remote sensing for mapping flooded areas. International Journal of Engineering Research and Application, 3(5), 1–5.

Ouma, Y. O., Tateishi, R. (2014). “Urban flood vulnerability and risk mapping using integrated multi-parametric AHP and GIS: Methodological overview and case study assessment”. Water(Switzerland), 6(6), 1515–1545. https://doi.org/10.3390/w606151

Oxford university. (2024). "oxford dictionaries language matters," oxford university press [Online]. Available: https://www.oxfordlearnersdictionaries.com/definition/american_english/flood_1

Poudel, K; Basne, K; Sherchan, B. (2021). “Hydrological and Hydraulic Modeling for Flood Analysis: A Case Study for Modi Catchment”. International journal of engineering research and technology, 10(8). http://doi:10.17577/IJERTV10IS080220

Pravat , J., Kasiviswanathan, K. S., & Soundharajan, B. (2023). An optimization approach for reducing the bias in standard plotting position methods. Developments in Environmental Science. (pp. 299-308) https://doi.org/10.1016/B978-0-443-18640-0.00001-8.

Renard, B; McInerney, D; Westra, S; Leonard, M; Kavetski, D; Thyer, M; Vidal, J. -P (2023). Floods and Heavy Precipitation at the Global Scale: 100-Year Analysis and 180-Year Reconstruction. Journal Of Geophysical Research: Atmospheres, http://doi:10.1029/2022jd037908

Righini, M.; Gatti, I.; Taramelli, A.; Arosio, M.; Valentini, E.; Sapio, S.; Schiavon, E. (2024). “Integrated Flood Impact and Vulnerability Assessment Using a Multi-Sensor Earth Observation

Mission with the Perspective of an Operational Service in Lombardy, Italy". Land, 13, 140. https://doi.org/10.3390/land13020140

Saikh, N. I., & Mondal, P. (2023). Gis-based machine learning algorithm for flood susceptibility analysis in the Pagla river basin, Eastern India. Natural Hazards Research. https://doi.org/10.1016/j.nhres.2023.05.004

Samarasinghea, S.; Nandalalb, H.; Weliwitiyac, D.; Fowzed, J.; Hazarikad, M.; Samarakoond, L. (2010). "Application of remote sensing and GIS for flood risk analysis: A case study at Kalu-Ganga River, Sri Lanka". Int. Arch. Photogramm. Remote Sensing Spatial Information Science, 38(8),110-115.

Samuel, G. (2021). "Flood risk assessment for pro-active response to flood disasters in Gaborone, Botswana". Msc thesis, University of Zambia; Lusaka Zambia. http://https://dspace.unza.zm/items/fc47767a-075c-45c8-9c42-c6faf8c3d199

Sanyal, J., Lu, X.X. (2004). "Application of Remote Sensing in Flood Management with Special Reference to Monsoon Asia: A Review". Natural Hazards 33, 283–301. https://doi.org/10.1023/B:NHAZ.0000037035.65105.95

Schumann, G. (2015). "Preface: Remote Sensing in Flood Monitoring and Management." Remote Sensing, 7(12), 17013–17015. https://doi.org/10.3390/rs71215871

Sebego, R. J., Atlhopheng, J. R., Chanda, R., Mulale, K., & Mphinyane, W. (2019). Land use intensification and implications on land degradation in the Boteti area: Botswana. African Geographical Review, 38(1), 32–47. https://doi.org/10.1080/19376812.2017.1284599

Sugianto, S.; Deli, A.; Miswar, E.; Rusdi, M.; Irham, M. (2022). "The Effect of Land Use and Land Cover Changes on Flood Occurrence in Teunom Watershed, Aceh Jaya". Land, 11, 1271. https://doi.org/10.3390/land11081271

Tasri, E. S; Karimi, K; Muslim, I. (2021). "The effect of economic variables on natural disasters and the impact of disasters on economic variables. Heliyon. 28;8(1):e08678. http://doi:10.1016/j.heliyon.2021.e08678

Townsend P. A. (2002). "Relationship between forest structure and the detection of flood inundation in forested wetlands using C-band SAR". International Journal of Remote Sensing, Vol. 23, No. 3, pp. 443–460. http://DOI:10.1080/01431160010014738

Townsend P. A., and Walsh S. J. (1998). Modelling floodplain inundation using an integrated GIS with radar and optical remote sensing. Geomorphology, Vol. 21, pp. 295-312. https://doi.org/10.1016/S0169-555X(97)00069

UN-ISDR (International Strategy for Disaster Reduction). (2008). "Living with risk. A global review of disaster reduction initiatives." Inter-Agency Secretariat of the international strategy for disaster reduction. http://https://www.unisdr.org/files/657_lwr1.pdf

UNISDR. (2015). “The human cost of weather related disaster”, United Nations, Geneva. https://www.unisdr.org/files/46796_cop21weatherdisastersreport2015.pdf

Wagenaar D, Curran A, Balbi M, Bhardwaj A, Soden R, Hartato E, Mestav Sarica G, Ruangpan L, Molinario G, Lallemant D (2020) Invited perspectives: how machine learning will change flood risk and impact assessment. Nat Hazards Earth Syst Sci 20:1149–1161. https://doi.org/10.5194/nhess-20-1149-2020

World Meteorological Organization. (2013) "Integrated Flood Management Tools Series No.20 flood mapping," Associated Programme on Flood Management, Switzerland.

Yang, X.; Chu, Q.; Wang, L.; Yu, M. (2022). Water Body Super-Resolution Mapping Based on Multiple Endmember Spectral Mixture Analysis and Multiscale Spatio-Temporal Dependence. Remote Sens. https://doi.org/10.3390/rs14092050

Zhai, L.; Lee, J. E. (2023). “Harnessing ICT Resources to Enhance Community Disaster Resilience: A Case Study of Employing Social Media to Zhengzhou 7.20 Rainstorm, China”. Water, 15, 3516. https://doi.org/10.3390/w15193516